Analysing Amazonian Forest Productivity Using a new Individual & Trait -Based Model (TFS v.1).

Nikolaos M Fyllas[1*], Emanuel Gloor[1], Lina M Mercado[2], Stephen Sitch[2], Carlos A Quesada[3], Tomas F Domingues[4], David R. Galbraith[1], Armando Torre-Lezama[5], Emilio Vilanova[5], Hirma Ramírez-Angulo[5], Niro Higuchi[3], David A. Neill[6], Marcos Silveira[7], Leandro Ferreira[8], Yadvinder Malhi[9], Oliver L Phillips[1] and Jon Lloyd[10,11].

1. Ecology and Global Change, School of Geography, University of Leeds, UK
2. School of Geography, University of Exeter, UK
3. Instituto Nacional de Pesquisas da Amazônia, Manaus, Brazil
4. School of GeoSciences, University of Edinburgh, Scotland, UK
5. Instituto de Investigaciones para el Desarrollo, Forestal Facultad de Ciencias Forestales y Ambientales, Universidad de Los Andes, Venezuela
6. Department of Wildlife Conservation and Management, Universidad Estatal Amazónica, Puyo, Pastaza, Ecuador 7. Universidade Federal do Acre, Rio Branco, Brazil
8. Museu Paraense Emílio Goeldi, Belém, Brazil
9. Environmental Change Institute, School of Geography and the Environment, University of Oxford, UK
10. Centre for Tropical Environmental and Sustainability Science (TESS) and School of Marine and Tropical Biology, James Cook University, Australia
11. Department of Life Sciences, Imperial College London, Silwood Park Campus, Ascot, UK.
** Currently at: Department of Ecology & Systematics, Faculty of Biology, University of Athens, Greece.*

Abstract

Repeated long-term censuses have revealed large-scale spatial patterns in Amazon Basin forest structure and dynamism, with some forests in the west of the Basin having up to a twice as high rate of aboveground biomass production and tree recruitment as forests in the east. Possible causes for this variation could be the climatic and edaphic gradients across the Basin and/or the spatial distribution of tree species composition. To help understand causes of this variation a new individual-based model of tropical forest growth, designed to take full advantage of the forest census data available from the Amazonian Forest Inventory Network (RAINFOR), has been developed. The model allows for within-stand variations in tree size distribution and key functional traits and between-stand differences in climate and soil physical and chemical properties. It runs at the stand level with four functional traits, leaf dry mass per area (M_a), leaf nitrogen (N_L) and phosphorus (P_L) content and wood density (D_W) varying from tree to tree in a way that replicates the observed continua found within each stand. We first applied the model to validate canopy-level water fluxes at three eddy covariance flux measurement sites. For all three sites the canopy-level water fluxes were adequately simulated. We then applied the model at seven plots, where intensive measurements of carbon allocation are available. Tree-by-tree multi-annual growth rates generally agreed well with observations for small trees, but with deviations identified for larger trees. At the stand-level, simulations at 40 plots were used to explore the influence of climate and soil nutrient availability on the gross (Π_G) and net (Π_N) primary production rates as well as the carbon use efficiency (C_U). Simulated Π_G, Π_N and C_U were not associated with temperature. On the other hand, all three measures of stand level productivity were positively related to both mean annual precipitation and soil nutrient status. Sensitivity studies showed a clear importance of an

accurate parameterisation of within- and between-stand trait variability on the fidelity of model predictions. For example, when functional tree diversity was not included in the model (i.e., with just a single plant functional type with mean Basin-wide trait values) the predictive ability of the model was reduced. This was also the case when Basin-wide (as opposed to site-specific) trait distributions were applied within each stand. We conclude that models of tropical forest carbon, energy and water cycling should strive to accurately represent observed variations in functionally important traits across the range of relevant scales.

Keywords: Amazon Basin, tropical forest, individual-based model, functional traits, stomatal conductance, soil nutrient availability, gross primary productivity, net primary productivity, carbon use efficiency.

Author for correspondence: Nikolaos M. Fyllas, nfyllas@gmail.com

1. Introduction

The Amazon Basin, encompassing one of the planet's largest forest areas and hosting one quarter of the Earth's biodiversity, constitutes a large reservoir of living biomass (Malhi and Phillips, 2005). Amazon forests also have a substantial influence on regional and global climates (Shukla et al. 1990; Spracklen et al., 2012). These forests are, however, under strong human pressure through logging, forest to pasture conversion, and face at present a warming and more variable climate and changing atmospheric composition (Lewis et al., 2004; Gloor et al., 2013). Due to the enormous area of forest within the Amazon Basin, these factors have the potential to modify global atmospheric greenhouse concentrations, regional and global climate, and the overall biodiversity of the planet (Cramer et al., 2004).

Traditionally, two approaches have been followed to understand current and future state of the Amazon forests. First, Dynamic Global Vegetation Models (DGVM) have been used to simulate vegetation patterns and carbon fluxes across Amazonia (Moorcroft et al., 2001; Galbraith et al., 2010) with some predicting substantial carbon losses under scenarios of global change (White et al., 1999; Cox et al., 2004) but with others less so (Cramer et al., 2004), or even gains (Huntingford et al., 2013). A second approach to understand Amazonian forests dynamics is through the analysis of long-term field observations of patterns of tree growth and mortality as they relate to climatic and edaphic variations across the Basin (e.g. Phillips et al., 2004; Quesada et al., 2012).

Analyses of Amazon forest inventory data, and particularly those of the Amazon Forest Inventory Network (RAINFOR) (Malhi et al., 2002), have revealed large-scale temporal trends in biomass and species composition as well as intriguing spatial patterns in many stand properties (Phillips et al., 1998; Baker et al., 2004, Phillips et al., 2009). Specifically, there is systematic spatial variation in species composition, biomass, growth and turnover rates, with western forests exhibiting higher wood productivity, faster turnover time and lower stand wood density compared to eastern forests (Baker et al., 2004; Malhi et al., 2006). This macroecological variation may possibly be explained by the Basin-wide observed climate and soil nutrient availability gradients (terSteege et al., 2006; Quesada et al., 2012). The climatic gradient comprises a southeast to northwest increase in annual precipitation and decrease in dry season length (Sombroek, 2001), with aboveground wood productivity positively related to precipitation (Malhi et al., 2004). On the other hand, a soil age/nutritional axis spans from the northeastern part of the basin to southwestern Amazonia, with generally younger and richer soils in the west and highly weathered nutrient poor soils in the east (Sombroek, 2000; Quesada et al., 2011), although at regional and local scales the patterns are often more complicated than this macro-gradient might imply (Higgins et al., 2011). Soil physical properties (such as rooting depth, drainage and water holding capacity and soil structure) are similarly related to soil age and parental material (Quesada et al., 2010). Poor physical (for example soil depth) conditions (less weathered soils) are often associated with higher soil nutrient availability (Walker and Syers, 1976; Vitousek and Farrington, 1997) leading to increased nutrient concentrations at the leaf level (Fyllas et al., 2009) and thus a potential for higher photosynthetic rates (Reich et al., 1994; Raaimakers et al., 1995). In addition, increased disturbance-associated mortality rates in soils of poor physical properties lend towards more dynamic stands where faster growing species dominate (Chao et al., 2009, Quesada et al., 2012). This positive feedback

97 mechanism could explain the higher aboveground productivity and turnover rates observed for western
98 forests (Quesada et al., 2012).

99 The simplistic ways by which plant functional diversity is currently reflected in DGVMs is an
100 important shortcoming in predicting ecosystem response to environmental gradients and their
101 vulnerability to global change (Lavorel et al., 2007). Some of the widely applied DGVMs represent
102 Amazonian plant diversity with only few plant functional types (PFT), for example the LPJ model uses
103 only two tropical-oriented PFTs (Sitch et al., 2003) and the JULES model only one (Clark et al., 2011).
104 The mean values of key model parameters like photosynthetic capacity, wood density and leaf turnover
105 times are selected to describe an *a priori* PFT definition (Fyllas et al., 2012). This means that many
106 processes are controlled by a set of fixed parameters that describe viable plant strategies within very
107 limited boundaries. Such PFT implementation has important drawbacks. It is usually based on the
108 average value of a plant trait recorded from different field studies and different species. But recent
109 studies have shown that key traits present a wide variation, dependent upon species identity and site
110 growing conditions (Sultan, 2000; Fyllas et al., 2009; Baraloto et al., 2010a). Thus any given species has
111 the potential to exhibit site-dependent shifts in its trait value; this being in addition to the inter-specific
112 trait variability expected at any given site. Ignoring this plasticity could potentially bias modelling
113 through an underestimation of the PFT's resilience by projecting dramatic but artificial switches in
114 vegetation state caused by the limited and discrete (step-wise) nature of PFT descriptions.

115 Such unaccounted variability could be particularly important when modelling Amazonian forest
116 dynamics, where environmental heterogeneity and plant functional diversity comprise key components
117 of the ecosystem (Townsend et al., 2008). For example, the variation in leaf mass per area (M_a)
118 recorded within Amazon forests covers an approximately similar range to the one identified in global
119 datasets, ranging from 30 to 300 gm^{-2} (Fyllas et al., 2009). Similarly, there are large contrasts in soil
120 physical and chemical conditions (Quesada et al., 2010). These important ecosystem flux drivers have
121 now been better quantified with Amazon-wide climate (Malhi and Wright, 2004), soil (Quesada et al.,
122 2011) and functional trait datasets also having been obtained (Baker et al., 2009; Fyllas et al., 2009;
123 Patiño et al., 2009; Patiño et al., 2012). This is in addition to continually expanding long-term forest
124 inventory data in which tree growth, mortality and species composition data are regularly being
125 recorded (Keeling et al., 2008; Chao et al., 2009).

126 We here introduce a vegetation dynamics model developed as a tool to better analyse these
127 observed Amazonian large-scale productivity patterns. This is achieved through specific incorporations
128 of observed environmental and the biotic variations into the model formulation. Specifically we focus
129 a) on the architectural variability, expressed through the size-class distribution of a stand, and b) on the
130 functional variability, expressed through simulated distributions of four important functional traits
131 which are allowed to vary from tree to tree within individual plots. Following a continuum approach,
132 we replace the use of a discrete number of PFTs, with distributions of a functional traits "quartet" the
133 within-stand distributions of which also vary from plot to plot in accordance with observation.

134 Two axes of functional variation/strategy are represented in the model: the leaf economic and
135 the tree architecture spectra. The four functional traits include leaf mass per area (M_a), leaf nitrogen and
136 phosphorous dry mass concentration (N_{Lm} and P_{Lm} respectively) and wood density (D_W). The first three

traits express one component of the leaf economic spectrum (Reich et al., 1997; Wright et al., 2004), i.e. a global photosynthetic tissue trade-off between inexpensive, short-lived and fast payback leaves *vs.* costly, long-lived and slow payback leaves; although we emphasise that other factors such as leaf cation concentrations may be important in this respect (Fyllas et al., 2012; Patiño et al., 2012). Low M_a and high nutrient content leaves are associated with comparably short longevity and usually have high (mass-based) gas exchange rates (Reich et al., 1994; Raaimakers et al., 1995). Lately the role of P_{Lm} has been highlighted as it expresses alternative limitations of the photosynthetic efficiency of tropical tree species (Domingues et al., 2010). The fourth trait, D_W, is used to represent a tree architectural axis with denser wood species supporting an overall higher aboveground biomass and thus having a higher maintenance respiration (Chave et al., 2005; Mori et al., 2010, although see Larjavaara and Muller-Landau, 2012). These two dimensions capture essentially a growth vs. survival trade-off. There is mixed evidence for a coordination between leaf and stem traits, i.e. a correlation between slow return related leaf traits and denser wood (Chave et al., 2009), with Baraloto et al. (2010b) suggesting that these two axes are independent, but with Patiño et al. (2012) showing some important correlations with foliar traits such as P_{Lm}. For the purpose of this study we consider leaf and stem dimensions as independent axes of tree functional variation, with no predefined interrelationship between the representative traits. However, the observed among-stand variability of these four characters is used to express how growing conditions control plant processes while the within-stand trait variation represents a range of ecological strategies found under the same growing conditions.

The model is initialised with site-specific tree diameter and functional traits data, and forced with daily climate data. We first test the ability of the model to estimate stand-level water fluxes at three eddy-flux tower sites. For a subset of seven RAINFOR plots where site-specific carbon allocation coefficients are known, a tree-level test of stem growth rates is applied. We further validate the ability of the model to simulate the spatial patterns of aboveground biomass productivity at 40 RAINFOR plots, and subsequently explore the variation of Gross Primary Productivity (Π_G), Net Primary Productivity (Π_N) and Carbon Use Efficiency (C_U) along established Amazonian climatic and edaphic gradients.

2. Materials and Methods

2.1 Model Description

"Traits-based Forest Simulator" (TFS) is an individual-based forest model, i.e. it simulates water and carbon fluxes for each tree in a stand. In the current version of the model, stand structure is prescribed in terms of the number of trees and their diameter at breast height (d). This is thus a "snapshot" version of the model, which does not take into account tree recruitment and mortality. In this version of TFS, each individual is fully described through d, with allometric equations used to estimate other attributes of interest like tree height (H), crown area (C_A), total leaf area (L_A) and tree-level leaf area index (L). Whole tree biomass is then partitioned to leaf (B_L), stem (B_S), coarse root (B_{CR}) and fine root (B_{FR}) biomass using established allometric equations. Allocation of assimilated carbon to different plant components is static, i.e. it does not change with size or resource availability, but rather implements field-derived allocation coefficients (Aragão et al., 2009). The general architecture of the model is presented in Fig. 1.

Tree functional diversity is expressed through four traits (M_a, N_{Lm}, P_{Lm}, D_W), which are randomly assigned to each tree: these pseudo-data being generated from local observations using a random vector generation algorithm. Leaf photosynthesis is calculated using a modified version of the Farquhar biochemical model (Farquhar et al., 1980), that incorporates leaf chemical and soil moisture effects. The maximum photosynthetic rate is regulated by N_L or P_L through the co-limitation model of Domingues et al. (2010). In contrast to most ecosystem fluxes models, where photosynthetic rates are directly regulated by water availability (Scheiter and Higgins, 2009; Clark et al. 2011), we couple water 'stress' to reduction of canopy conductance by estimating a daily fractional available soil water content for each tree in the stand. Carbon fluxes are simulated on an hourly and water fluxes on a daily time-step.

Light competition is based on the assumption of a perfect canopy tessellation. The flat-top version of the perfect plasticity model (Purves et al., 2007) has been used in the current version of TFS to characterise canopy and sub-canopy trees, by assuming that all of a tree's foliage is found at the top of its stem (S1, Canopy Architecture and Radiation Environment). A canopy height Z^* is estimated for each forest stand, defining canopy and sub-canopy trees. By summing up the crown area (C_A) of all trees in the stand, Z^* is estimated as the height of the last tree that enters to the sum before the cumulative crown area is equal to the plot area. Canopy trees are absorbing a mean daily amount of shortwave solar radiation equal to the sum of mean beam, diffuse and scattered daily radiation in correspondence to the sun-shade model of de Pury and Farquhar (1997). The direct and diffuse fraction of solar radiation is estimated using the Spitters et al. (1986) approximation. The functional configuration of a tree (i.e. the values of the traits quartet) does not affect its light competitive status, as tree height and crown area are not directly associated to any of the four traits. Future versions of the model will incorporate such effects.

Soil water balance is approximated through a simple bucket model, with soil water content affecting leaf conductance and thus photosynthetic rates. Competition for soil water is approximated through a size hierarchy, i.e. bigger trees, with a more extensive root system are assumed to have access to deeper water (S1, Water Balance Algorithm). By assuming that a tree with a higher leaf biomass (B_L) requires a higher fine root biomass (B_{FR}), we indirectly implement a M_a effect on water competition (S1, Definition, Allometry and Stoichiometry of Individual Trees in TFS). In particular, between two trees of the same size, the higher M_a tree will be more competitive in terms of acquiring soil water.

TFS is coded in Java and it is fully described in S1. The main effects of including functional diversity are realised through trait-driven effects on photosynthesis and respiration (Reich et al., 2008; Reich et al., 2009). Model components that are linked with any of the four base traits are described in following paragraphs. All statistical analyses and graphs were made with R (R Development Core Team, 2013).

2.1.1 Within-stand Functional Diversity

As noted above, TFS employs neither species nor PFT descriptions, but rather a different discrete combination of each the four key functional traits M_a, N_{Lm}, P_{Lm} and D_W is assigned to each individual tree along with a diameter-based allometry. To achieve this, the four functional characters assigned are generated using a procedure based on the actual values recorded within each plot. This is

achieved using a random vector generation algorithm (Taylor and Thompson, 1986). This algorithm, appropriate for generating non-repeated pseudo-observations from a relatively small sample of observations, was originally developed to provide for a realistic probabilistic representation of shrapnel projectile distributions in military battlefield simulations in the face of only a limited amount of available data (due to the cost and difficulty of undertaking the appropriate experiments). This "ballistic method" is notable in that it was specifically designed to short-circuit the usual step of multivariate density in the generation a pseudorandom population with approximately the same moments as the original sample. The ballistic method is readily programmable as follows (with the underlying rationale as discussed in Taylor & Thompson (1986) and Thompson (1989)) and with the following description based on Visual Numerics (2014):

First take a vector X with n multivariate observations (x_1…. x_n). To generate a pseudodataset $\tilde{x}$ from x, one observation (x_i) is first chosen at random and its nearest m neighbours, x_{j1}, x_{j2}, x_{jm} are then determined and with the mean $\overline{x_j}$ of those nearest neighbours subsequently calculated. Next, a random sample u_1, u_2, …, u_m is generated from a uniform distribution with lower bound $\frac{1}{m} - \sqrt{\frac{3(m-1)}{m^2}}$, and upper bound. $\frac{1}{m} + \sqrt{\frac{3(m-1)}{m^2}}$. The random variate $\tilde{x}_j$ is then the estimated as $\sum_{l=1}^{m} u_l \left(x_{jl} - \overline{x_j} \right) + \overline{x_j}$

and the process then repeated as required. Somewhat subjective here is the selection of the appropriate value of the number of nearest neighbours (m) although the nature of the simulations is not strongly dependent upon that value (Taylor & Thompson, 1986). Thus, following their recommendation and as in the Visual Numerics (2014) default, we have taken here $m = 5$.

In our case, applying this procedure resulted in a coordinated trait quartet for each tree in a stand being generated on the basis on the smaller observational trait quartets sampled from trees in the same stand (Baker et al., 2009; Fyllas et al., 2009; Patiño et al., 2012) and without any assumptions having to be made about their underlying statistical distributions. Thus no single functional trait "average stand" value is used (or even required). Further, between-stand differences in the traits distributions and their covariances are also intrinsically taken into account. This is because each stand is characterised by its own multivariate trait sample and size distribution. More fertile plots have an overall lower M_a and higher N_{Lm} and P_{Lm} compared to infertile plots (Fyllas et al., 2009), with this being reflected in the photosynthetic capacity of individual trees, as described in the next paragraph.

2.1.2 Photosynthesis

A tree-level leaf area index (L), estimated as the ratio of L_A to C_A, is used to compute the energy, carbon and water fluxes for each tree in a stand. The net photosynthetic rate (μmol m^{-2} s^{-1}) is given from:

$$A_n = g_s (C - C_i) \quad (1)$$

with C_α the atmospheric CO_2 mixing ratio (μmol mol^{-1}), C_c the CO_2 mixing ratio inside the chloroplast and g_s the CO_2 stomatal conductance (mol m^{-2} s^{-1}) calculated from Medlyn et al. (2011) and modulated by a soil moisture term. The leaf-level photosynthetic rate A_n is scaled-up to the tree-level by multiplying with the C_A of the tree.

The co-limitation equation suggested by Domingues et al. (2010), where the leaf level photosynthetic capacity (area basis) is potentially limited by either nitrogen or phosphorus is used TFS to estimate the leaf maximum carboxylation and electron transport rates:

$$V_{max} = M_a \left(\min \left\{ a_{NV} + v_{NV} N_{Lm}, a_{PV} + v_{PV} P_{Lm} \right\} \right) \quad (2)$$

$$J_{max} = M_a \left(\min \left\{ a_{NJ} + v_{NJ} N_{Lm}, a_{PJ} + v_{PJ} P_{Lm} \right\} \right) \quad (3)$$

both in (μmol m^{-2} s^{-1}), and a_{NV}, a_{NJ}, a_{PV}, a_{PJ} in (μmolg^{-1} s^{-1}) and v_{NV}, v_{NJ}, v_{PV}, v_{PJ} in (μmol mg^{-1} s^{-1}) empirical coefficients (see S1). The canopy-level photosynthetic capacity V_{Cmax}(μmol m^{-2} s^{-1}) is estimated using the tree-level leaf area index L, taking into account within canopy gradients in light and photosynthetic capacity based on Lloyd et al. (2010). Nutrient optimisation is approximated using equations in Lloyd et al. (2010), with M_a also dependent on the height of each tree (H_i) and the mean canopy height ($\overline{H_S}$):

$$M_a^* = M_a \cdot \exp\left[a_H \cdot (H_i - \overline{H_S}) \right] \quad (4), \text{ with } a_H \text{ an empirical coefficient.}$$

2.1.2 Respiration

Tree respiration includes a growth and a maintenance component, both computed daily. Growth respiration is considered as a constant fraction (0.25) of daily photosynthesis (Cannell and Thornley, 2000). Three different maintenance respiration formulations are allowed in TFS (S1, Respiration), but in this study we use the one described below. Leaf maintenance respiration R_{mL} is estimated as a fraction of V_{Cmax} (Scheiter and Higgins, 2009):

$$R_{mL} = 0.015 V_{Cmax} \quad (5)$$

Stem maintenance respiration is estimated from the sapwood volume (V_S) of a tree:

$$R_{mS} = \delta V_S \quad (6), \text{ with } \delta = 39.6 \text{ (μmol } m^{-3} \text{ } s^{-1}) \text{ as reported in Ryan et al. (1994) for tropical trees.}$$

Sapwood volume is estimated by inversing the pipe model and assuming that the ratio of leaf area to sapwood area (Φ_{LS}) increases with the height and the wood density for tropical trees following (Calvo-Alvarado et al., 2008; Meinzer et al., 2008):

$$\Phi_{LS} = 0.5 \times (\lambda_1 + \lambda_2 \cdot H + \delta_1 + \delta_2 D_W) \quad (7),$$

with λ_1=0.066 m^2 cm^{-2}, λ_2=0.017 m cm^{-2}, δ_1= - 0.18 m^2 cm^{-2} and δ_2=1.6 cm^3 g^{-1}.

Sapwood area (m^2) and volume (m^3) are then calculated from:

$S_A = L_A / \Phi_{LS}$ (8), with L_A the total leaf area of the tree (m^2) and

$S_V = S_A \cdot (H - C_D)$ (9), with C_D the crown depth (m)

Coarse root maintenance respiration R_{mCR} is estimated as in Scheiter and Higgins (2009):

$$R_{mCR} = 0.218 \beta_R \frac{B_{CR}}{\Phi_{CN}} \quad (10)$$

where Φ_{CN} is the root C:N ratio estimated on the basis of the simulated N_R assuming a dry weight carbon fraction of 0.5.

Fine root maintenance respiration R_{mFR} is assumed to be equal to leaf respiration.

All respiratory components are corrected with the temperature dependence function of Tjoelker et al. (2001). The total maintenance respiration R_m is then:

$R_m = R_{mL} + R_{mS} + R_{mCR} + R_{mFR}$ (11)

2.1.3 Stomatal Conductance

Initially, a maximum (no water stress) stomatal conductance, $g_{s,max}$ is calculated following Medlyn et al. (2011, 2012):

$$g_{s,max} = g_0 + 1.6 \cdot \left(1 + \frac{g_1}{\sqrt{D_C}}\right) \times \frac{A_n}{C_a} \quad (12)$$

with g_0 (mol m^{-2} s^{-1}) the minimum stomatal conductance, g_1(-) an empirical coefficient that represents the water use efficiency of the plant, and D_C the leaf-to-atmosphere vapour pressure difference. Values of g_0 and g_1 that lead to the best model performance were different between sites, as indicated by the model calibration procedure. For the basin-wide simulations constant values of g_0=0.020 (mol m^{-2} s^{-1}) and g_1=5.0 (-) were used, close to the estimates of Domingues et al. (2014). In future versions of the model, we anticipate that g_0 and g_1 will be related to other functional traits. The maximum stomatal conductance is subsequently reduced to the actual g_s by multiplying the second term of equation 8 with a water stress coefficient.

In contrast to most ecosystem fluxes model, where photosynthetic rates are directly regulated by water availability (Scheiter and Higgins, 2009; Clark et al. 2011), we couple soil water deficit to canopy conductance by estimating a daily fractional available soil water content ϑ_i, for each i tree in the stand (S1, Water Balance and Soil Water Stress). This term is then used to estimate the water stress γ_i that has a direct effect on stomatal conductance, as also described in Keenan et al. (2010).

306 **2.2 Study Sites & Simulations Set-up**

307 Three sets of site data were used to explore the behaviour of the model. These include a set of
308 three eddy flux measurements (EFM) sites, seven plots with intensive carbon balance and allocation
309 measurements (IM), and 40 permanent measurement plots (PM).

310 **2.2.1 Eddy flux (EFM) sites**

311 Daily climate and energy flux data from three EFM sites (Caxiuanã [1.72S, 51.46W], Manaus
312 [2.61S, 60.21W] and Tapajós [2.86S, 54.96W]) were used to assess the ability of the model to estimate
313 canopy-level water fluxes. Data were obtained from the Large Scale Biosphere-Atmosphere
314 Experiment in Amazonia (LBA) project (http://daac.ornl.gov/LBA/lba.shtml). In particular mean
315 daily climate parameters including incoming radiation, temperature, precipitation, relative humidity and
316 wind speed were used to force the model. Latent heat flux (λE in Wm^{-2}) was used to estimate a daily
317 mean canopy conductance defined as $G_C = \frac{\lambda E}{D_C}$. The EFM data cover a period from 2001 to 2008 for
318 Caxiuanã, from 2000 to 2005 for Manaus and from 2002 to 2004 for Tapajós. *Gc* was only estimated
319 for days with a complete diurnal record of λE. At each one of the EFM sites the mean daily *Gc* (mol m^{-2}
320 s^{-1}) was compared between observations and simulations. The model was initialized with size-class
321 distribution and functional traits data from RAINFOR permanent plots located near the eddy flux
322 towers. Specifically, CAX-06 inventory data were used for Caxiuanã, BNT-04 for Manaus, and TAP-55
323 for Tapajós. We note that the EFM sites are mainly found at the eastern part of Amazonia (Fig. 2)
324 growing on low nutrient status soils.

325 The model was initially calibrated to the site specific values for g_0 and g_1 of equation 8 that gave
326 the best performance. A Standardised Major Axis (SMA) regression, forced through zero was used to
327 verify the ability of the model to simulate *Gc*, with a regression slope close to one indicating a good
328 model performance.

329 **2.2.2 Intensive measurement (IM) sites**

330 The ability of the model to realistically simulate carbon fluxes at the tree-level is evaluated using
331 data from the seven intensive measurement plots (Aragão et al., 2009; Malhi et al., 2009). These sites
332 are amongst the intensively surveyed plots within the RAINFOR network (Fig. 2), where
333 measurements of all major components of the C cycle are recorded (Malhi et al., 2009). At these plots, a
334 detailed assessment of the carbon stocks is applied, and Π_N allocation coefficients to different plant
335 components are estimated (Aragão et al., 2009; Malhi et a. 2011; Doughty et al., 2013). These site-
336 specific coefficients are used to calculate the amount of simulated Π_N that is allocated to stems $\Pi_{N,s}$
337 (kgC y^{-1}).

338 The IM sites of interest include two plots at Agua Pudre in Colombia (AGP-01 & AGP-02), one
339 (ALP-30) at Allpahuayo/Peru, one (BNT-04) at Manaus/Brazil, one in Caxiuanã /Brazil (CAX-06), one
340 in Tambopata/Peru (TAM-05) and one in (TAP-55) Tapajós /Brazil. Based on data from Quesada et
341 al. (2011), AGP-01, AGP-02, TAM-05 can be considered to be located on fertile soils, with the other

four plots on infertile ones. Available soil depth data (Quesada et al., 2011) and functional traits data (Fyllas et al., 2009) were used for site specific simulations. For all seven sites we estimated the observed average multi-annual growth rate (2000-2006) of each tree from forest census data, in order to compare it with the simulated $\Pi_{N,s}$.

The daily climate was extracted from the Princeton Global Meteorological Forcing Dataset (Sheffield et al., 2006). These simulations are used to validate the ability of the model to accurately estimate tree-level stem growth, under a given stand structure, a given climatic and soil profile and functional traits configuration of the established trees. Average observed stem growth rate (per 10 cm *d* bins), expressed in carbon units(i.e. kg C y^{-1}), is compared with simulated $\Pi_{N,s}$ using the York method of best straight line, which holds when both x and y observations are subject to correlated errors that vary from point to point (York et al., 2004).

2.2.3 Permanent measurement (PM) sites

Inventory data from 40 RAINFOR permanent measurement plots (Fig. 2), including tree diameter and multiannual growth for all trees greater than 10 cm curated/managed in ForestPlots.net (Lopez-Gonzalez et al., 2009; Lopez-Gonzalez et al., 2011), are used to a) validate the ability of the model to accurately simulate stand-level carbon fluxes and b) explore patterns of Π_G, Π_N and C_U along the Amazonian climatic and soil nutrient availability gradient. The size class distribution within each PM site is used to initialise the stand structure of the model and simulate patterns of productivity for the 2000-2006 period. Climate data for the same period were used here with the first year again used as a spin-up period (Sheffield et al., 2006). For those 40 PM plots, sample distributions of the traits quartet are available (Fyllas et al., 2009) as well as a description of soil chemical and physical properties (Quesada et al., 2011).

At the PM sites the simulated stand-level aboveground Π_N was compared with observed rates of aboveground growth (ΔB_{ABG} ($kgCm^{-2}$ y^{-1})) for trees that survived during the 2000-2006 time period using a SMA regression. A second step was to explore the way Π_G, Π_N and C_U vary across an Amazon climatic and soil nutrient availability gradient (Quesada et al., 2010). The site scores of a principal components analysis (PCA) on the soil properties of the 40 PM plots (see Fyllas et al., 2009) are used to categorise plots along a nutrient availability gradient (Φ_1), while the key climatic variables used were the annual mean temperature T_A and annual total precipitation P_A. A Kendall correlation coefficient (τ) was used to identify potential relationships of Π_G, Π_N and C_U with T_A, P_A and Φ_1, as in most cases non-linear associations were observed.

2.2.4 Randomisation Exercise

In order to explore a) the importance of including trait variability and thus functional diversity in our simulations and b) the importance of including constrains that are known to control the large scale patterns of Amazonian forest dynamics, we conducted a randomisation exercise with the model beeing run under four alternative set-ups at the 40 permanent RAINFOR plots. The first set-up denoted as *var-tr* is the variable-trait simulation with trait initialization based on the observed stand-level trait distribution as described in the previous paragraphs (default set-up). The second set-up, denoted as *fix-*

tr, is a fixed-trait simulation with all trees having the same (dataset mean) values for each trait: This thus representing a single PFTs case. The third set-up (*rand-tr*) is a variable-trait simulation with trait initialization based on random values of the traits quartet as recorded in any individual along the 40 permanent plots. This setup thus ignores any potential patterns of functional trait biogeography, i.e. traits are not related to the environmental or edaphic conditions under which a tree is growing. The fourth setup *(rand-tr-N*) is a variable trait simulation where the photosynthetic capacity of an individual is only defined by its leaf N content and thus the NP co-limitation constraint is removed. These alternative set-ups were compared by considering both the slope and the R^2 of SMA regressions between the predicted and the observed $\Pi_{N,S}$.

3. Results

3.1 Canopy conductance simulations at the EFM sites

Values of best model performance for g_0 and g_1 were different between sites, with g_0=0.035 (mol m^{-2} s^{-1}) and g_1=7.5 at Caxiuanã, g_0=0.035 and g_1=7.0 at Manaus with g_0=0.01 and g_1=2.5 these being somewhat lower than the estimates of Domingues et al. (2013) at Tapajós. Simulated *G*c was underestimated for Caxiuana (α=0.85±0.05) and Manaus (α=0.90±0.02), with the model overestimating *G*c in Tapajos (α=1.28±0.04), but exhibiting an overall adequate performance (Fig. 3). For simulations at the IM and the PM sites, constant values of g_0=0.02 (mol m^{-2} s^{-1}) and g_1=5 (-) were used, which are found within the range of values in the EFM sites and reported estimates (Medlyn et al. 2012; Domingues et al., 2013).

3.2 Stem growth rate simulations at the IM sites

The mean simulated stem growth rate $\Pi_{N,s}$ of each tree in the seven IM plots was compared with the observed aboveground biomass gains (ΔB_{ABG}) for the 2000-2006 period. An accurate simulation of $\Pi_{N,s}$ can be seen for small size classes, but with greater differences between the observed and the simulated multi-annual growth found for bigger trees (Fig. 4). At infertile ALP-30, the estimate slope of the York model indicated an overestimation of aboveground production (α=1.18±0.06), driven mainly by an overestimation of the mid-size classes. At BNT-04 the model underestimated the overall growth (α=0.82±0.03). Aboveground growth was overestimated in CAX-06 (1.11±0.07). At TAP-55 (α=1.44±0.15) the model underestimated aboveground production (0.90±0.06). At fertile AGP-01 (α=1.36±0.08) and AGP-02 (α=1.25±0.05) an overestimation of aboveground productivity was observed although with simulations of most size classes falling within the observed ranges. At TAM-05 (α=0.79±0.07) though, the simulated aboveground growth was underestimated with the overall slope driven by divergences in smaller size classes. The range and distribution of Π_N allocation to stem growth is adequately captured by TFS as summarised in Fig B1.

3.3 GPP, NPP and CUE simulations at the PM sites

Simulated stand-level aboveground net primary productivity $\Pi_{N,A}$ was positively associated with observed changes in aboveground biomass of trees that survived in the PM plots over the 2000-2006 period ΔB_{ABG}, with an R^2=0.42, suggesting an adequate model behaviour (Fig. 5). A summary of simulated stand-level Π_G, Π_N and C_U relationship to key environmental drivers is given in Table 1 (see also Fig B2). Π_G and Π_N and C_U were not associated with temperature. However, all three measures of stand level productivity were positively related to annual precipitation and soil nutrient availability.

3.4 Randomisation Exercise Simulations

Results from the randomisation exercise (Fig. 6) found the fully constrained default set-up (*var-tr*) to have the best predictive performance (R^2=0.42 with a SMA slope a=0.92). This is as compared to the fixed trait simulations (*fix-tr*) single PFT parameterization with a decreased predictive ability of TFS (R^2=0.29, a=0.82) and an overall higher mean predicted aboveground productivity. Not accounting for the site specific distribution of the traits quartet, i.e. bypassing potential biogeographic patterns of functional diversity and/or environmental-trait interactions (*rand-tr*) also reduced the predictive ability of the model (R^2=0.29, a=0.74). Finally the random trait no NP co-limitation set-up (*rand-tr-N*) similarly lead to an inferior model performance (R^2=0.33, a=0.88) and with the highest mean simulated aboveground productivity.

4. Discussion

We report here on the core components of an individual-based model that has been developed in order to help better understand the patterns revealed by recent integrated measurements of climate, soils, functional diversity and stand dynamics for a wide range of forests across the Amazon Basin. In its current setup the model does not explicitly simulate regeneration and mortality dynamics but rather uses the observed size distribution of trees at the study sites, thus taking into account stand structure and functional trait variability as observed along the main climatic and edaphic axes of the Amazon Basin. With the current setup we were able to reproduce the tree- and stand- level Π_N patterns found across Amazonia and to explore for potential environmental controls over stand-level Π_G, Π_N and C_U.

4.1 Scientific Outcomes

Our simulations found no association of stand level *gross primary productivity* (Π_G) with temperature, probably due to the relatively small range of variation of temperature across our plots. Π_G decreased until an annual temperature of approximately 26°C but remained relative constant above this point (Table 1, Fig. A.2.2). However, our simulations suggest that a strong association of Π_G with the annual precipitation and soil nutrient availability of the plots. Π_G was positively related to annual precipitation over the entire range observed in the 40 PM plots. The association of Π_G with the nutrient availability axis is in agreement with fertilisation experiments showing an increase with nutrient supply (Giardina et al., 2003). In our Basin-wide examination of Π_G the soil nutrient availability and

stand structure gradients are not, however, independent (Quesada et al., 2012), as in the RAINFOR network permanent plots it has been observed that bigger/older trees are more abundant on eastern infertile forests, where soil physical conditions can support a bigger tree size (Baker et al., 2009) with a lower risk of trees being uprooted (Chao et al., 2009). Bigger trees generally support a greater foliage area and thus could significantly contribute to the overall carbon assimilation of the stand. However, bigger trees on infertile plots are generally characterised by lower leaf nutrient concentrations (Fyllas et al., 2009) and thus slower assimilation rates (Reich et al., 1994; Domingues et al., 2010). On the other hand a higher abundance of smaller trees with higher gas exchange rates is observed on more dynamic, fertile plots. Ultimately this indicates that stand structure should be specifically taken into account when simulating Π_G in tropical forests, and thus individual-based models could significantly contribute towards a deeper understanding of the functioning and sensitivity of these ecosystems.

In our simulations stand-level *net primary productivity* (Π_N) showed no significant association to annual temperature but increased with soil nutrient availability and annual precipitation (Table 1, Fig. A.2.2). Our Π_N simulations are in agreement with field observations of increasing aboveground wood productivity with precipitation (Quesada et al., 2012). Based on TFS parameterisation, photosynthetic rates are expected to be higher at a greater soil nutrient availability due to associated higher leaf N and P concentration (Fyllas et al., 2009; Domingues et al., 2010). Using a similar parameterisation for a "sun and shade" big leaf model, Mercado et al. (2011) found an increase in net canopy assimilation rate with leaf P content in agreement with our positive association between Π_N and soil nutrient availability. Their simulated Π_G accounted for approximately 0.30 of the observed wood productivity in 33 study plots, and thus the R^2=0.42 between simulated Π_N and aboveground growth found here suggest a marginally improved model behaviour. It should be noted that our definition of soil nutrient availability (Φ_1), based on the PCA analysis in Quesada et al. (2010), directly relates to soil P content. As shown first in the analysis of Quesada et al. (2012), where data from almost 60 plots were considered, aboveground Π_N is positively related to soil P content in lowland tropical forest. The increased Π_N in fertile environments (apart from the higher Π_G) seems to be enhanced by the greater abundance of small trees there. As tree size increases maintenance respiration likely "consumes" an increasing proportion of assimilated carbon, and thus at large size classes the proportion of trees which have enough carbon to allocate to growth decreases (Givnish, 1988; Cavaleri et al., 2008). This is in line with the negative relationship between coarse wood production and maximum height documented for some Amazonian trees (Baker et al., 2009).

In our simulations c*arbon use efficiency* (C_U) ranged from 0.43 to 0.54. Recent research suggests that the C_U is not as constant as had been previously suggested (De Lucia et al., 2007; Zhang et al., 2009). For example the meta-analysis of De Lucia et al. (2007) found that C_U varies from 0.23 to 0.83 in different forest types. Our average estimate of C_U=0.51 is, however, above the range of reported in Malhi (2012). Zhang and colleagues (2009) identified a negative trend of the Π_N/Π_G ratio with temperature at the range of 20 to 30 °C, as also simulated here especially above 26°C (Fig A2.2). Simulated C_U increased with soil nutrient availability, being marginally lower at infertile (0.48) compared to fertile (0.50) plots. This is attributable to smaller size class trees (with lower relative respiratory costs) constituting a greater proportion of the total stand biomass on higher nutrient status soils. One factor relating to soil nutrient availability but not included in the current version is an implicit consideration of the respiratory costs of plant nutrient uptake (Lambers et al., 2008) either directly, or through other

processes such as organic acid exudation (Jones et al., 2009) or the symbiotic associations (Duponnois et al., 2012.) One would expect these costs to be proportionally higher for stand of a low nutrient status, especially with regard to P (Quesada et al., 2012).

4.2 Practical implications

The modelling of tropical forest carbon fluxes and stand dynamics has traditionally involved approaches aimed at a balance between simplicity, computational economy, and complexity. On one hand, the enormous biological and biogeochemical heterogeneity of tropical forests (Townsend et al., 2008) places special importance on how modelers prioritise both the amount and the detail of processes that should be included to capture the main controls and feedbacks. On the other hand, the finding that Amazonia is dominated by just 227 tree species (ter Steege et al., 2013) implies that most biogeochemical cycling in the world's largest tropical forest is performed by a tiny sliver of its diversity. At one end of the complexity spectrum are individual-based models which are able to properly simulate population dynamics and thus lags due to demography. Individual-based models of tropical forests have traditionally focused on realistically representing the light environment (TROLL - Chave, 1999) or grouping tree species on the basis of their different responses to environmental resources as suggested by field observations (FORMIND - Kohler & Huth, 1998, LPJ-GUESS – Helly et al., 2006). At the other end of the complexity spectrum are DGVMs which simulate population dynamics more simplistically (but see Moorcroft et al., 2001; Scheiter & Higgins, 2009). Using a DGVM model Verheijen et al. (2013) allowed for within-PFT climate-driven trait variation to occur and achieved an improvement of the predicted vegetative biomass and PFT distribution patterns. A similar rationale was followed in Wang et al. (2012) where it was shown that the inclusion of multi-trait covariance in DGVM can be used to constrain model parameters and reduce uncertainties in simulated ecosystem productivity. Fisher et al. (2010) applied the individual-based Ecosystem Demography model (Moorcroft et al., 2001), and showed that by varying traits related to demographic processes, forest and biomass dynamics exhibited a wide range of responses to climate forcing.

Most of the above approaches have used discrete PFTs to represent tree species and functional diversity. These studies suggest that by allowing for within PFT trait variability a more plastic and realistic response to the relevant environmental drivers is observed. In contrast to the above, TFS replaces the use of PFTs with traits distributions, following a different model philosophy and architecture using the concept of multidimensional trait continua. In particular, considering functional diversity to be expressed by a multidimensional trait space, the use of PFTs selects a number of clusters where the central vector defines the average trait values of each PFT (Fyllas et al., 2012). Recent studies (Verheijen et al., 2013; Wang et al., 2012) allow for the average trait values to be shifted based on empirical climatic and/or trait inter-correlation functions. In contrast, the use of trait continua does not cluster the multidimensional trait space but rather allows any realistic trait combination (as suggested by the limited sampling of the actual population) to be simulated. Successful trait combinations under given environmental conditions may then be expected to emerge as a by-product of model dynamics (Higgins et al., 2014). A similar to TFS representation of functional diversity has been implemented in the aDGVM model (Scheiter & Higgins, 2009; Scheiter et al., 2013) where the importance of including trait-variability in simulations of vegetation dynamics has also been highlighted. In TFS, variable-trait (R^2=0.42) simulations led to a better model performance compared to fixed-trait (R^2=0.29) simulations

(Fig. 6). Thus including functional diversity in simulations of vegetation dynamics is expected not only to suggest less vulnerable communities under changing climatic conditions (Fauset et al., 2012; Scheiter et al., 2013) but also, it seems, to better describe the current patterns of key ecosystem properties like aboveground productivity.

A few modelling studies that implement a similar traits continua approach have recently been published. Scheiter & Higgins (2009) were the first to develop an individual-based framework that eschews the use of PFTs and allows for plants to allocate carbon as a function of local environmental conditions. Falster and colleagues (2011) presented a model where they used leaf economic strategy, height, wood density and seed size to scale-up from individual scale processes to landscape predictions. Pavlick et al. (2013) applied an interesting approach where they used 15 traits to incorporate trait diversity within plant community in a DGVM. The rationale of the above models is that they allow different plant functional strategies to be available in a specific location with given environmental conditions (for example a grid cell), and that by setting up a set of functional trade-offs they "filter out" poorly adapted trait combinations from the community. This is effectively an implementation of ideas arising from the environmental filtering/community assembly theory to predict an optimum plant community at a given location (Keddy, 1992; Scheiter et al., 2013; Fortunel et al., 2014). By contrast, drawing on recent findings on the processes controlling Amazonian forest dynamics, we have here attempted to incorporate within TFS the relevant observed associations between functional trait diversity, stand-structure and soil physical and chemical properties (Fyllas et al., 2009, Quesada et al., 2012). Although there are similarities with some of the more recent models discussed above to our knowledge this is the first time all these linkages have been represented in a single modelling framework. Our approach has been made possible (and thus differs from others) because of the type and quantity of observational constraints used. For example in any given plot we do not force the model to select some "optimum" trait combination based on the prevailing environmental conditions, but we rather assume that the observed trait distribution reflects that of the evolutionary stable community structure occurring at each site. Similarly we don't require the model to predict what the optimum tree-size class distribution would be. Rather, we initialize simulations with what is observed. We have here employed this implementation as our primarily aim in this first instance has been to validate the predictive ability of the model at some extensively monitored Amazonian plots.

Even with these prescribed constraints, the trait randomization exercise yielded some interesting outputs regarding the importance of trait variability in simulations of forest dynamics. As already discussed the default variable-trait (*var-tr*) simulations gave the best TFS performance in terms of predicting patterns of aboveground production at the 40 permanent measurement plots with fixed trait (*fix-tr*) TFS simulations showing a lower predictive ability and an overall higher mean Π_{AN}. This pattern of trait variability reducing above-ground biomass is in contrast with a similar simulation from Scheiter et al. (2013), where variable trait simulations gave rise to a higher mean biomass because of an increased chance of selecting a trait combination allowing trees to grow larger. This difference arises from the photosynthesis NP co-limitation constraint hardwired into the current version of TFS as the use of the Amazon wide mean N_L and P_L values, leads inevitably to universally phosphorus limited estimates of V_{cmax} and J_{max} that reduce the overall predictive ability of the model. Indeed, when the NP co-limitation is removed, the variable trait simulations (*rand-tr-N*) do actually yield the highest Π_{AN} estimates. Finally the random variable trait setup (*rand-tr*) resulted again in a similarly poor TFS

behavior (R^2=0.29), emphasizing the importance of potential environment – trait interactions in accounting for between-stand structural differences. In other words, in the modelling tropical forest dynamics it is clear that trait distributions cannot be used without a consideration of how they may be shifted by the local growing conditions.

The four functional traits used in the current version of TFS, i.e. leaf dry mass per area, leaf nitrogen and phosphorous concentrations and wood density, are directly related to the rates of tree photosynthesis and respiration. For that reason they provide a stable basis that should allow alternative ecological strategies based on well known trade-offs such as the "growth vs. survival" to be implemented in trait-based vegetation dynamics models. These four traits have been extensively studied around 70 plots in the Amazon and their patterns of variation and inter-correlation have been analysed (Baker et al., 2009; Fyllas et al., 2009; Patiño et al., 2009; Patiño et al., 2012). For the purpose of this study, it is important to know the within stand variation of the functional traits used, i.e. the trait values at the individual level across different plots. Additional functional traits that were considered but not included as base traits in this version of TFS were the seed size and the leaf area to sapwood area ratio. Seed size is an important functional trait that expresses a tolerance vs. fecundity trade-off, with seed size trading-off with seed number and with larger seed species being more tolerant at more stressful places (Muller-Landau, 2010). However, data on seed size are usually available at the species level, i.e. intraspecific variation is not usually recorded, and thus this kind of data cannot be included in the current version of TFS. The leaf area to sapwood area ratio, Φ_{LS}, is an important trait that can be used to constrain the hydraulic architecture of trees (Meinzer et al., 2008). Here Φ_{LS} is expressed as a function of D_W and H (equation 7) and it is not used as an independent (base) trait. Future version of TFS will include this aspect of functional variability, but for this first study we have selected just a small set of key traits in order to maintain a relative simple model structure.

Like most modelling efforts, TFS represents work in progress. We identify three particularly promising avenues for future improvements. Firstly, discrepancies between the observed and simulated stem level growth rates, particularly in larger size classes, could result from the allometric equations used to estimate aboveground biomass and growth not being species or size specific. The allometric equations used here express a generic height *(H) vs. d* relationship for Amazonia, without taking into account habitat and species differences, so a more accurate representation of tree architecture would probably result in better biomass growth estimation. Indeed, *H-d* relationships do vary significantly among species (King, 1996; Poorter et al., 2006) and across regions (Nogueira et al., 2008; Feldpausch et al., 2011; Goodman et al., 2013). An additional source of bias when estimating stem-level growth rates could be related to the uniform (static) allocation coefficient used in this study. For example, Litton et al. (2007) showed that allocation to aboveground tree biomass components increases with age and the availability of resources. Furthermore, Castanho et al. (2013) improved the predictions of a DGVM by adjusting allocation coefficients based on soil texture. Such ontogenetic and/or resource based shifts in patterns of carbon allocation could be potentially modelled through the use of dynamic allocation schemes (Friedlingstein et al., 1999; Franklin et al., 2012).

The importance of realistically representing autotrophic respiration processes in models of vegetation dynamics is also highlighted here. Modelling respiration has proven to be a difficult task (Cannell and Thornley, 2000), and accurately representations of this component is of great importance

for understanding the global C cycle (Valentini et al., 2000). For example the way respiration is represented in DGVMs could have a substantial control over the way the dynamics of Amazonian forest under scenarios of climatic change are simulated (Huntingford et al., 2004; Galbraith et al., 2010). Nitrogen content of plant tissue has been proven a good predictor of respiration rates (Reich et al., 2008). However, Mori et al. (2010) suggested a mixed-power equation where the exponent varies from 1 to 3/4 as size increases. Both the Reich and Mori models are implemented in TFS, but we found that a third method, combining the size and nitrogen control, performed better. Thus we suggest that an amalgamation of those two approaches could provide a better way to estimate respiration fluxes in the new generation of dynamic vegetation models. In addition leaf phosphorous content seems to constrain respiration rates stronger than nitrogen content in some tropical forests (Meir et al., 2001; Meir and Grace, 2002), and thus inclusion of a phosphorus constraint in future equations of leaf respiration could increase their realism.

Finally, discrepancies in the observed versus the simulated canopy conductance G_C could result from the parameterisation of the stomata conductance model of Medlyn et al. (2011). The estimates for g_0 and g_1 used in the 40 PM plots simulations were taken as constant. However, Medlyn et al. (2011) suggested that g_0 and g_1 could vary with functional group. Thus the Amazon wide parameterisation used here should be replaced with local level estimates when appropriate gas exchange data are available, and ultimately with estimates based on linked functional traits as evidenced through recently documented associations between structural characteristics such as wood density and leaf area: sapwood ratio with leaf physiological traits such as M_a and leaf $^{13}C/^{13}C$ ratio (Patiño et al., 2012), although we also note that the extent of such structural/physiological linkages remains the subject of debate (Baraloto et al., 2010b). Alternative stomatal closure equations as a function of soil water availability (Harris et al. 2004) should also be tested along with the conductance model in future versions of the model.

5. Conclusions

We set out to develop a modelling framework for tropical forests that is relatively simple yet adequately complex to capture the main ecological gradients in the world's most extensive tropical forest. Our study places special emphasis on processes highlighted by recent field studies to strongly influence Amazonian forest dynamics, especially functional trait diversity and its association with multiple soil properties (Fyllas et al., 2009). In summary TFS is characterised by a relatively simple setup, which is capable to reproduce water and carbon fluxes as observed at both daily and multi-annual time scales. TFS represents an important link between inventory data, and large scale models with the incorporation of the continuum of plant strategies, through the inclusion of trait distributions providing a step towards better representing diversity in vegetation modelling (Lavorel et al., 2007), representing important processes and trait variation that cannot be adequately accounted for by a DGVM approach to vegetation modelling. Since TFS is based heavily on measured data, the model is well suited to testing hypotheses related to the present day Amazon biogeography and biogeochemical fluxes.

6. Code availability

The JAVA source code can be obtained upon request. Contact: nfyllas@gmail.com

Acknowledgments

This research was supported by a Marie Curie Intra-European Fellowship within the 7th European Community Framework Programme to NM Fyllas. Manuel Gloor and Lina Mercado were funded by the AMAZONICA NERC consortium grant. OP is supported by an ERC Advanced Grant and (as for JL) a Royal Society Wolfson Research Merit Award. The work of RAINFOR between 2000 and 2006 was supported primarily by the UK Natural Environment Research Council and the European Community Framework Programme through grants to OP, YM, and JL. Natalia Restrepo Coupe provided the gap filled eddy flux tower data. Gabriela Lopez-Gonzalez and Sophie Fauset helped with data preparation. The Missouri Botanical Garden, Rodolfo Vasquez, Abel Monteagudo, Nigel Pitman, Adriana Prieto, Agustin Rudas, Natalino Silva, Gerardo Aymard, Chiqui Arroyo and Alejandro Araujo Murakami contributed permanent plot data to the RAINFOR network.

References

Aragão, L. E. O. C., Malhi, Y., Metcalfe, D. B., Silva-Espejo, J. E., Jiménez, E., Navarrete, D., Almeida, S., Costa, A. C. L., Salinas, N., Phillips, O. L., Anderson, L. O., Alvarez, E., Baker, T. R., Goncalvez, P. H., Huamán-Ovalle, J., Mamani-Solórzano, M., Meir, P., Monteagudo, A., Patiño, S., Peñuela, M. C., Prieto, A., Quesada, C. A., Rozas-Dávila, A., Rudas, A., Silva Jr., J. A. and Vásquez, R.: Above- and below-ground net primary productivity across ten Amazonian forests on contrasting soils, Biogeosciences, 6(12), 2759–2778, 2009.

Baker, T. R., Phillips, O. L., Laurance, W. F., Pitman, N. C. A., Almeida, S., Arroyo, L., DiFiore, A., Erwin, T., Higuchi, N., Killeen, T. J., Laurance, S. G., Nascimento, H., Monteagudo, A., Neill, D. A., Silva, J. N. M., Malhi, Y., López Gonzalez, G., Peacock, J., Quesada, C. A., Lewis, S. L. and Lloyd, J.: Do species traits determine patterns of wood production in Amazonian forests?, Biogeosciences, 6(2), 297–307, 2009.

Baker, T. R., Phillips, O. L., Malhi, Y., Almeida, S., Arroyo, L., Fiore, A. D., Erwin, T., Higuchi, N., Killeen, T. J., Laurance, S. G., Laurance, W. F., Lewis, S. L., Monteagudo, A., Neill, D. A., Vargas, P. N., Pitman, N. C. A., Silva, J. N. M. and Martínez, R. V.: Increasing biomass in Amazonian forest plots, Phil. Trans. R. Soc. Lond. B, 359(1443), 2004.

Baraloto, C., Timothy Paine, C. E., Patino, S., Bonal, D., Herault, B. and Chave, J.: Functional trait variation and sampling strategies in species-rich plant communities, Functional Ecology, 24(1), 208–216, 2010a.

Baraloto, C., Timothy Paine, C. E., Poorter, L., Beauchene, J., Bonal, D., Domenach, A.M., Hérault, B., Patiño, S., Roggy, J.-C. and Chave, J.: Decoupled leaf and stem economics in rain forest trees, Ecology Letters, 13(11), 1338–1347, 2010b.

Calvo-Alvarado, J. C., McDowell, N. G. and Waring, R. H.: Allometric relationships predicting foliar biomass and leaf area: sapwood area ratio from tree height in five Costa Rican rain forest species, Tree physiology, 28(11), 1601–1608, 2008.

Cannell, M. G. R. and Thornley, J. H. M.: Modelling the components of plant respiration: some guiding principles, Annals of Botany, 85(1), 45–54, 2000.

Castanho, A. D. A., Coe, M. T., Costa, M. H., Malhi, Y., Galbraith, D. and Quesada, C. A.: Improving simulated Amazon forest biomass and productivity by including spatial variation in biophysical parameters, Biogeosciences, 10(4), 2255–2272, 2013.

Cavaleri, M. A., Oberbauer, S. F. and Ryan, M. G.: Foliar and ecosystem respiration in an old-growth tropical rain forest, Plant, Cell & Environment, 31(4), 473–483, 2008.

Chao, K.-J., Phillips, O. L., Monteagudo, A., Torres-Lezama, A. and Vásquez Martínez, R.: How do trees die? Mode of death in northern Amazonia, Journal of Vegetation Science, 20(2), 260–268, 2009.

Chave, J.: Study of structural, successional and spatial patterns in tropical rain forests using TROLL, a spatially explicit forest model, Ecological Modelling, 124(2), 233–254, 1999.

Chave, J., Andalo, C., Brown, S., Cairns, M. A., Chambers, J. Q., Eamus, D., Fölster, H., Fromard, F., Higuchi, N., Kira, T., Lescure, J.-P., Nelson, B. W., Ogawa, H., Puig, H., Riéra, B. and Yamakura, T.:

704 Tree allometry and improved estimation of carbon stocks and balance in tropical forests, Oecologia,
705 145(1), 87–99, 2005.

706 Chave, J., Coomes, D., Jansen, S., Lewis, S. L., Swenson, N. G. and Zanne, A. E.: Towards a worldwide
707 wood economics spectrum, Ecology Letters, 12(4), 351–366, 2009.

708 Clark, D. B., Mercado, L. M., Sitch, S., Jones, C. D., Gedney, N., Best, M. J., Pryor, M., Rooney, G. G.,
709 Essery, R. L. H., Blyth, E., Boucher, O., Harding, R. J., Huntingford, C. and Cox, P. M.: The Joint UK
710 Land Environment Simulator (JULES), model description – Part 2: Carbon fluxes and vegetation
711 dynamics, Geoscientific Model Development, 4(3), 701–722, 2011.

712 Cox, P. M., Betts, R. A., Collins, M., Harris, P. P., Huntingford, C. and Jones, C. D.: Amazonian forest
713 dieback under climate-carbon cycle projections for the 21st century, Theoretical and Applied
714 Climatology, 78(1-3), 137–156, 2004.

715 Cramer, W., Bondeau, A., Schaphoff, S., Lucht, W., Smith, B. and Sitch, S.: Tropical forests and the
716 global carbon cycle: impacts of atmospheric carbon dioxide, climate change and rate of deforestation,
717 Philosophical Transactions of the Royal Society of London. Series B: Biological Sciences, 359(1443),
718 331–343, 2004.

719 DeLucia, E., Drake, J. E., Thomas, R. B. and Gonzalez-Meller, M.: Forest carbon use efficiency: is
720 respiration a constant fraction of gross primary production?, Global Change Biology, 13(6), 1157–1167,
721 2007.

722 Domingues, T. F., Martinelli, L. A. and Ehleringer, J. R.: Seasonal patterns of leaf-level photosynthetic
723 gas exchange in an eastern Amazonian rain forest, Plant Ecology & Diversity, 7(1-2), 189–203, 2014.

724 Domingues, T. F., Meir, P., Feldpausch, T. R., Saiz, G., Veenendaal, E. M., Schrodt, F., Bird, M.,
725 Djagbletey, G., Hien, F., Compaore, H., Diallo, A., Grace, J. and Lloyd, J.: Co-limitation of
726 photosynthetic capacity by nitrogen and phosphorus in West Africa woodlands, Plant, Cell &
727 Environment, 33(6), 959–980, 2010.

728 Doughty, C. E., Metcalfe, D. B., da Costa, M. C., de Oliveira, A. A. R., Neto, G. F. C., Silva, J. A.,
729 Aragão, L. E. O. C., Almeida, S. S., Quesada, C. A., Girardin, C. A. J., Halladay, K., da Costa, A. C. L.
730 and Malhi, Y.: The production, allocation and cycling of carbon in a forest on fertile terra preta soil in
731 eastern Amazonia compared with a forest on adjacent infertile soil, Plant Ecology & Diversity, 7(1-2),
732 41–53, 2014.

733 Duponnois, R., Baudoin, E., Thioulouse, J., Hafidi, M., Galiana, A., Lebrun, M. and Prin, Y.: The
734 Impact of Mycorrhizosphere Bacterial Communities on Soil Biofunctioning in Tropical and
735 Mediterranean Forest Ecosystems, in Bacteria in Agrobiology: Plant Probiotics, edited by D. K.
736 Maheshwari, pp. 79–95, Springer Berlin Heidelberg, 2012.

737 Falster, D. S., Brännström, AAke, Dieckmann, U. and Westoby, M.: Influence of four major plant traits
738 on average height, leaf-area cover, net primary productivity, and biomass density in single-species
739 forests: a theoretical investigation, Journal of Ecology, 99(1), 148–164, 2011.

740 Farquhar, G. D., von Caemmerer, S. von and Berry, J. A.: A biochemical model of photosynthetic CO2
741 assimilation in leaves of C3 species, Planta, 149(1), 78–90, 1980.

742 Fauset, S., Baker, T. R., Lewis, S. L., Feldpausch, T. R., Affum-Baffoe, K., Foli, E. G., Hamer, K. C.
743 and Swaine, M. D.: Drought-induced shifts in the floristic and functional composition of tropical
744 forests in Ghana, Ecology letters, 15(10), 1120–1129, 2012.

745 Feldpausch, T. R., Banin, L., Phillips, O. L., Baker, T. R., Lewis, S. L., Quesada, C. A., Affum-Baffoe,
746 K., Arets, E. J. M. M., Berry, N. J., Bird, M., Brondizio, E. S., de Camargo, P., Chave, J., Djagbletey, G.,
747 Domingues, T. F., Drescher, M., Fearnside, P. M., França, M. B., Fyllas, N. M., Lopez-Gonzalez, G.,
748 Hladik, A., Higuchi, N., Hunter, M. O., Iida, Y., Salim, K. A., Kassim, A. R., Keller, M., Kemp, J.,
749 King, D. A., Lovett, J. C., Marimon, B. S., Marimon-Junior, B. H., Lenza, E., Marshall, A. R., Metcalfe,
750 D. J., Mitchard, E. T. A., Moran, E. F., Nelson, B. W., Nilus, R., Nogueira, E. M., Palace, M., Patiño, S.,
751 Peh, K. S.-H., Raventos, M. T., Reitsma, J. M., Saiz, G., Schrodt, F., Sonké, B., Taedoumg, H. E., Tan,
752 S., White, L., Wöll, H. and Lloyd, J.: Height-diameter allometry of tropical forest trees, Biogeosciences,
753 8(5), 1081–1106, 2011.

754 Fisher, R., McDowell, N., Purves, D., Moorcroft, P., Sitch, S., Cox, P., Huntingford, C., Meir, P. and
755 Ian Woodward, F.: Assessing uncertainties in a second-generation dynamic vegetation model caused by
756 ecological scale limitations, New Phytologist, 187(3), 666–681, 2010.

757 Fortunel, C., Paine, C. E., Fine, P. V., Kraft, N. J. and Baraloto, C.: Environmental factors predict
758 community functional composition in Amazonian forests, Journal of Ecology, 102(1), 145–155, 2014.

759 Franklin, O., Johansson, J., Dewar, R. C., Dieckmann, U., McMurtrie, R. E., Brännström, \AAke and
760 Dybzinski, R.: Modeling carbon allocation in trees: a search for principles, Tree physiology, 32(6), 648–
761 666, 2012.

762 Friedlingstein, P., Joel, G., Field, C. B. and Fung, I. Y.: Toward an allocation scheme for global
763 terrestrial carbon models, Global Change Biology, 5(7), 755–770, 1999.

764 Fyllas, N. M., Patiño, S., Baker, T. R., Nardoto, G. B., Martinelli, L. A., Quesada, C. A., Paiva, R.,
765 Schwarz, M., Horna, V., Mercado, L. M., Santos, A., Arroyo, L., Jimenez, E. M., Luizao, F. J., Neill, D.
766 A., Silva, N., Prieto, A., Rudas, A., Silviera, M., Vieira, I. C. G., Lopez-Gonzalez, G., Malhi, Y., Phillips,
767 O. L. and Lloyd, J.: Basin-wide variations in foliar properties of Amazonian forest: phylogeny, soils and
768 climate, Biogeosciences, 6, 2677–2708, 2009.

769 Fyllas, N. M., Quesada, C. A. and Lloyd, J.: Deriving plant functional types for Amazonian forests for
770 use in vegetation dynamics models, Perspectives in Plant Ecology, Evolution and Systematics, 14(2),
771 97–110, 2012.

772 Galbraith, D., Levy, P. E., Sitch, S., Huntingford, C., Cox, P., Williams, M. and Meir, P.: Multiple
773 mechanisms of Amazonian forest biomass losses in three dynamic global vegetation models under
774 climate change, New Phytologist, 187(3), 647–665, 2010.

775 Giardina, C. P., Ryan, M. G., Binkley, D. and Fownes, J. H.: Primary production and carbon allocation
776 in relation to nutrient supply in a tropical experimental forest, Global Change Biology, 9(10), 1438–
777 1450, 2003.

778 Givnish, T. J.: Adaptation to sun and shade: a whole-plant perspective, Functional Plant Biology, 15(2),
779 63–92, 1988.

780 Gloor, M., Brienen, R. J. W., Galbraith, D., Feldpausch, T. R., Schöngart, J., Guyot, J.-L., Espinoza, J.
781 C., Lloyd, J. and Phillips, O. L.: Intensification of the Amazon hydrological cycle over the last two
782 decades, Geophysical Research Letters, 2013.

783 Goodman, R. C., Phillips, O. L. and Baker, T. R.: The importance of crown dimensions to improve
784 tropical tree biomass estimates, Ecological Applications, doi:10.1890/13-0070.1, 2013.

785 Harris, P. P., Huntingford, C., Cox, P. M., Gash, J. H. and Malhi, Y.: Effect of soil moisture on canopy
786 conductance of Amazonian rainforest, Agricultural and Forest Meteorology, 122(3), 215–227, 2004.

787 Hély, C., Bremond, L., Alleaume, S., Smith, B., Sykes, M. T. and Guiot, J.: Sensitivity of African biomes
788 to changes in the precipitation regime, Global Ecology and Biogeography, 15(3), 258–270, 2006.

789 Higgins, M. A., Ruokolainen, K., Tuomisto, H., Llerena, N., Cardenas, G., Phillips, O. L., Vásquez, R.
790 and Räsänen, M.: Geological control of floristic composition in Amazonian forests, Journal of
791 biogeography, 38(11), 2136–2149, 2011.

792 Higgins, S. I., Langan, L. and Scheiter, S.: Progress in DGVMs: a comment on" Impacts of trait
793 variation through observed trait–climate relationships on performance of an Earth system model: a
794 conceptual analysis" by Verheijen et al.(2013), Biogeosciences Discussions, 11(3), 4483–4492, 2014.

795 Huntingford, C., Harris, P. P., Gedney, N., Cox, P. M., Betts, R. A., Marengo, J. A. and Gash, J. H. C.:
796 Using a GCM analogue model to investigate the potential for Amazonian forest dieback, Theoretical
797 and Applied Climatology, 78(1-3), 177–185, 2004.

798 Huntingford, C., Zelazowski, P., Galbraith, D., Mercado, L. M., Sitch, S., Fisher, R., Lomas, M.,
799 Walker, A. P., Jones, C. D., Booth, B. B. B., Malhi, Y., Hemming, D., Kay, G., Good, P., Lewis, S. L.,
800 Phillips, O. L., Atkin, O. K., Lloyd, J., Gloor, E., Zaragoza-Castells, J., Meir, P., Betts, R., Harris, P. P.,
801 Nobre, C., Marengo, J. and Cox, P. M.: Simulated resilience of tropical rainforests to CO2-induced
802 climate change, Nature Geosci, 6(4), 268–273, 2013.

803 Jones, D. L., Nguyen, C. and Finlay, R. D.: Carbon flow in the rhizosphere: carbon trading at the soil–
804 root interface, Plant and Soil, 321(1-2), 5–33, 2009.

805 Keddy, P. A.: Assembly and response rules: two goals for predictive community ecology, Journal of
806 Vegetation Science, 3(2), 157–164, 1992.

807 Keeling, H. C., Baker, T. R., Martinez, R. V., Monteagudo, A. and Phillips, O. L.: Contrasting patterns
808 of diameter and biomass increment across tree functional groups in Amazonian forests, Oecologia,
809 158(3), 521–534, 2008.

810 Keenan, T., Sabate, S. and Gracia, C.: Soil water stress and coupled photosynthesis–conductance
811 models: Bridging the gap between conflicting reports on the relative roles of stomatal, mesophyll
812 conductance and biochemical limitations to photosynthesis, Agricultural and Forest Meteorology,
813 150(3), 443–453, 2010.

814 King, D. A.: Allometry and life history of tropical trees, Journal of tropical ecology, 12(1), 25–44, 1996.

815 Köhler, P. and Huth, A.: The effects of tree species grouping in tropical rainforest modelling:
816 Simulations with the individual-based model FORMIND, Ecological Modelling, 109(3), 301–321, 1998.

817 Lambers, H., Raven, J. A., Shaver, G. R. and Smith, S. E.: Plant nutrient-acquisition strategies change
818 with soil age, Trends in Ecology & Evolution, 23(2), 95–103, 2008.

819 Larjavaara, M. and Muller-Landau, H. C.: Still rethinking the value of high wood density, American
820 Journal of Botany, 99(1), 165–168, 2012.

821 Lavorel, S., Díaz, S., Cornelissen, J. H. C., Garnier, E., Harrison, S. P., McIntyre, S., Pausas, J. G.,
822 Pérez-Harguindeguy, N., Roumet, C. and Urcelay, C.: Plant functional types: are we getting any closer
823 to the Holy Grail?, in Terrestrial ecosystems in a changing world, pp. 149–164, Springer, 2007.

824 Lewis, S. L., Phillips, O. L., Baker, T. R., Lloyd, J., Malhi, Y., Almeida, S., Higuchi, N., Laurance, W. F.,
825 Neill, D. A., Silva, J. N. M., Terborgh, J., Lezama, A. T., Martinez, R. V., Brown, S., Chave, J., Kuebler,
826 C., Vargas, P. N. and Vinceti, B.: Concerted changes in tropical forest structure and dynamics: evidence
827 from 50 South American long-term plots, Phil. Trans. R. Soc. Lond. B, 359(1443), 421–436, 2004.

828 Litton, C. M., Raich, J. W. and Ryan, M. G.: Carbon allocation in forest ecosystems, Global Change
829 Biology, 13(10), 2089–2109, 2007.

830 Lloyd, J., Patiño, S., Paiva, R. Q., Nardoto, G. B., Quesada, C. A., Santos, A. J. B., Baker, T. R., Brand,
831 W. A., Hilke, I., Gielmann, H., Raessler, M., Luizão, F. J., Martinelli, L. A. and Mercado, L. M.:
832 Optimisation of photosynthetic carbon gain and within-canopy gradients of associated foliar traits for
833 Amazon forest trees, Biogeosciences, 7(6), 1833–1859, 2010.

834 Lopez-Gonzalez, G., Lewis, S. L., Burkitt, M. and Phillips, O. L.: ForestPlots. net: a web application
835 and research tool to manage and analyse tropical forest plot data, Journal of Vegetation Science, 22(4),
836 610–613, 2011.

837 Lopez-Gonzalez, G., Lewis, S.L., Burkitt, M., Baker T.R. and Phillips, O.L. ForestPlots.net
838 Database.www.forestplots.net. Date of extraction [10,09,2013]

839 Malhi, Y.: The productivity, metabolism and carbon cycle of tropical forest vegetation, Journal of
840 Ecology, 100(1), 65–75, 2012.

841 Malhi, Y., Aragão, L. E. O. C., Metcalfe, D. B., Paiva, R., Quesada, C. A., Almeida, S., Anderson, L.,
842 Brando, P., Chambers, J. Q., Da COSTA, A. C. L., Hutyra, L. R., Oliveira, P., Patiño, S., Pyle, E. H.,
843 Robertson, A. L. and Teixeira, L. M.: Comprehensive assessment of carbon productivity, allocation and
844 storage in three Amazonian forests, Global Change Biology, 15(5), 1255–1274, 2009.

845 Malhi, Y., Doughty, C. and Galbraith, D.: The allocation of ecosystem net primary productivity in
846 tropical forests, Philosophical Transactions of the Royal Society B: Biological Sciences, 366(1582),
847 3225–3245, 2011.

848 Malhi, Y. and Phillips, O.: Tropical forests & global atmospheric change, Cambridge Univ Press, 2005.

849 Malhi, Y., Phillips, O. l., Lloyd, J., Baker, T., Wright, J., Almeida, S., Arroyo, L., Frederiksen, T., Grace,
850 J., Higuchi, N., Killeen, T., Laurance, W. f., Leaño, C., Lewis, S., Meir, P., Monteagudo, A., Neill, D.,
851 Núñez Vargas, P., Panfil, S. n., Patiño, S., Pitman, N., Quesada, C. a., Rudas-Ll., A., Salomão, R.,
852 Saleska, S., Silva, N., Silveira, M., Sombroek, W. g., Valencia, R., Vásquez Martínez, R., Vieira, I. c. g.
853 and Vinceti, B.: An international network to monitor the structure, composition and dynamics of
854 Amazonian forests (RAINFOR), Journal of Vegetation Science, 13(3), 439–450, 2002.

855 Malhi, Y., Wood, D., Baker, T. R., Wright, J., Phillips, O. L., Cochrane, T., Meir, P., Chave, J., Almeida,
856 S., Arroyo, L., Higuchi, N., Killeen, T. J., Laurance, S. G., Laurance, W. F., Lewis, S. L., Monteagudo,
857 A., Neill, D. A., Vargas, P. N., Pitman, N. C. A., Quesada, C. A., Salomão, R., Silva, J. N. M., Lezama,
858 A. T., Terborgh, J., Martínez, R. V. and Vinceti, B.: The regional variation of aboveground live biomass
859 in old-growth Amazonian forests, Global Change Biology, 12(7), 1107–1138, doi:10.1111/j.1365-
860 2486.2006.01120.x, 2006.

861 Malhi, Y. and Wright, J.: Spatial patterns and recent trends in the climate of tropical rainforest regions,
862 Philosophical Transactions of the Royal Society of London. Series B: Biological Sciences, 359(1443),
863 311–329, 2004.

864 Medlyn, B. E., Duursma, R. A., Eamus, D., Ellsworth, D. S., Colin Prentice, I., Barton, C. V., Crous, K.
865 Y., Angelis, P., Freeman, M. and Wingate, L.: Corrigendum for: "Reconciling the optimal and empirical
866 approaches to modelling stomatal conductance", Global Change Biology, 18(11), 3476–3476, 2012.

867 Medlyn, B. E., Duursma, R. A., Eamus, D., Ellsworth, D. S., Prentice, I. C., Barton, C. V., Crous, K. Y.,
868 de Angelis, P., Freeman, M. and Wingate, L.: Reconciling the optimal and empirical approaches to
869 modelling stomatal conductance, Global Change Biology, 17(6), 2134–2144, 2011.

870 Meinzer, F. C., Campanello, P. I., Domec, J.-C., Gatti, M. G., Goldstein, G., Villalobos-Vega, R. and
871 Woodruff, D. R.: Constraints on physiological function associated with branch architecture and wood
872 density in tropical forest trees, Tree Physiology, 28(11), 1609–1617, 2008.

873 Meir, P. and Grace, J.: Scaling relationships for woody tissue respiration in two tropical rain forests,
874 Plant, Cell & Environment, 25(8), 963–973, 2002.

875 Meir, P., Grace, J. and Miranda, A. C.: Leaf respiration in two tropical rainforests: constraints on
876 physiology by phosphorus, nitrogen and temperature, Functional Ecology, 15(3), 378–387, 2001.

877 Mercado, L. M., Patiño, S., Domingues, T. F., Fyllas, N. M., Weedon, G. P., Sitch, S., Quesada, C. A.,
878 Phillips, O. L., Aragão, L. E. O. C., Malhi, Y., Dolman, A. J., Restrepo-Coupe, N., Saleska, S. R., Baker,
879 T. R., Almeida, S., Higuchi, N. and Lloyd, J.: Variations in Amazon forest productivity correlated with
880 foliar nutrients and modelled rates of photosynthetic carbon supply, Phil. Trans. R. Soc. B, 366(1582),
881 3316–3329, 2011.

882 Moorcroft, P. R., Hurtt, G. C. and Pacala, S. W.: A method for scaling vegetation dynamics: the
883 ecosystem demography model (ED), Ecological monographs, 71(4), 557–586, 2001.

884 Mori, S., Yamaji, K., Ishida, A., Prokushkin, S. G., Masyagina, O. V., Hagihara, A., Hoque, A. T. M. R.,
885 Suwa, R., Osawa, A., Nishizono, T., Ueda, T., Kinjo, M., Miyagi, T., Kajimoto, T., Koike, T., Matsuura,
886 Y., Toma, T., Zyryanova, O. A., Abaimov, A. P., Awaya, Y., Araki, M. G., Kawasaki, T., Chiba, Y. and
887 Umari, M.: Mixed-power scaling of whole-plant respiration from seedlings to giant trees, PNAS, 107(4),
888 1447–1451, 2010.

889 Muller-Landau, H. C.: The tolerance–fecundity trade-off and the maintenance of diversity in seed size,
890 Proceedings of the National Academy of Sciences, 107(9), 4242–4247, 2010.

891 Nogueira, E. M., Fearnside, P. M., Nelson, B. W., Barbosa, R. I. and Keizer, E. W. H.: Estimates of
892 forest biomass in the Brazilian Amazon: New allometric equations and adjustments to biomass from
893 wood-volume inventories, Forest Ecology and Management, 256(11), 1853–1867, 2008.

894 Patiño, S., Fyllas, N. M., Baker, T. R., Paiva, R., Quesada, C. A., Santos, A. J. B., Schwarz, M., Steege,
895 H. ter, Phillips, O. L. and Lloyd, J.: Coordination of physiological and structural traits in Amazon forest
896 trees, Biogeosciences, 9(2), 775–801, 2012.

897 Patiño, S., Lloyd, J., Paiva, R., Baker, T. R., Quesada, C. A., Mercado, L. M., Schmerler, J., Schwarz, M.,
898 Santos, A. J. B., Aguilar, A., Czimczik, C. I., Gallo, J., Horna, V., Hoyos, E. J., Jimenez, E. M.,
899 Palomino, W., Peacock, J., Peña-Cruz, A., Sarmiento, C., Sota, A., Turriago, J. D., Villanueva, B.,
900 Vitzthum, P., Alvarez, E., Arroyo, L., Baraloto, C., Bonal, D., Chave, J., Costa, A. C. L., Herrera, R.,
901 Higuchi, N., Killeen, T., Leal, E., Luizão, F., Meir, P., Monteagudo, A., Neil, D., Núñez-Vargas, P.,
902 Peñuela, M. C., Pitman, N., Priante Filho, N., Prieto, A., Panfil, S. N., Rudas, A., Salomão, R., Silva, N.,
903 Silveira, M., Soares deAlmeida, S., Torres-Lezama, A., Vásquez-Martínez, R., Vieira, I., Malhi, Y. and
904 Phillips, O. L.: Branch xylem density variations across the Amazon Basin, Biogeosciences, 6(4), 545–
905 568, 2009.

906 Pavlick, R., Drewry, D. T., Bohn, K., Reu, B. and Kleidon, A.: The Jena Diversity-Dynamic Global
907 Vegetation Model (JeDi-DGVM): a diverse approach to representing terrestrial biogeography and
908 biogeochemistry based on plant functional trade-offs, Biogeosciences, 10(6), 4137–4177, 2013.

909 Phillips, O. L., Aragão, L. E. O. C., Lewis, S. L., Fisher, J. B., Lloyd, J., López-González, G., Malhi, Y.,
910 Monteagudo, A., Peacock, J., Quesada, C. A., Heijden, G. van der, Almeida, S., Amaral, I., Arroyo, L.,
911 Aymard, G., Baker, T. R., Bánki, O., Blanc, L., Bonal, D., Brando, P., Chave, J., Oliveira, Á. C. A. de,
912 Cardozo, N. D., Czimczik, C. I., Feldpausch, T. R., Freitas, M. A., Gloor, E., Higuchi, N., Jiménez, E.,
913 Lloyd, G., Meir, P., Mendoza, C., Morel, A., Neill, D. A., Nepstad, D., Patiño, S., Peñuela, M. C.,
914 Prieto, A., Ramírez, F., Schwarz, M., Silva, J., Silveira, M., Thomas, A. S., Steege, H. ter, Stropp, J.,
915 Vásquez, R., Zelazowski, P., Dávila, E. A., Andelman, S., Andrade, A., Chao, K.-J., Erwin, T., Fiore, A.
916 D., C, E. H., Keeling, H., Killeen, T. J., Laurance, W. F., Cruz, A. P., Pitman, N. C. A., Vargas, P. N.,
917 Ramírez-Angulo, H., Rudas, A., Salamão, R., Silva, N., Terborgh, J. and Torres-Lezama, A.: Drought
918 Sensitivity of the Amazon Rainforest, Science, 323(5919), 1344–1347, 2009.

919 Phillips, O. L., Baker, T. R., Arroyo, L., Higuchi, N., Killeen, T. J., Laurance, W. F., Lewis, S. L., Lloyd,
920 J., Malhi, Y., Monteagudo, A., Neill, D. A., Vargas, P. N., Silva, J. N. M., Terborgh, J., Martínez, R. V.,
921 Alexiades, M., Almeida, S., Brown, S., Chave, J., Comiskey, J. A., Czimczik, C. I., Fiore, A. D., Erwin,
922 T., Kuebler, C., Laurance, S. G., Nascimento, H. E. M., Olivier, J., Palacios, W., Patiño, S., Pitman, N.
923 C. A., Quesada, C. A., Saldias, M., Lezama, A. T. and Vinceti, B.: Pattern and process in Amazon tree
924 turnover, 1976–2001, Phil. Trans. R. Soc. Lond. B, 359(1443), 381–407, 2004.

925 Phillips, O. L., Malhi, Y., Higuchi, N., Laurance, W. F., Núñez, P. V., Vásquez, R. M., Laurance, S. G.,
926 Ferreira, L. V., Stern, M., Brown, S. and Grace, J.: Changes in the Carbon Balance of Tropical Forests:
927 Evidence from Long-Term Plots, Science, 282(5388), 439–442, 1998.

928 Poorter, L., Bongers, L. and Bongers, F.: Architecture of 54 moist-forest tree species: traits, trade-offs,
929 and functional groups, Ecology, 87(5), 1289–1301, 2006.

930 Purves, D. W., Lichstein, J. W. and Pacala, S. W.: Crown plasticity and competition for canopy space: a
931 new spatially implicit model parameterized for 250 North American tree species, PLoS One, 2(9), e870,
932 2007.

933 Pury, D. de and Farquhar, G. D.: Simple scaling of photosynthesis from leaves to canopies without the
934 errors of big-leaf models, Plant, Cell & Environment, 20(5), 537–557, 1997.

935 Quesada, C. A., Lloyd, J., Anderson, L. O., Fyllas, N. M., Schwarz, M. and Czimczik, C. I.: Soils of
936 Amazonia with particular reference to the RAINFOR sites, Biogeosciences, 8(6), 1415–1440,
937 doi:10.5194/bg-8-1415-2011, 2011.

938 Quesada, C. A., Lloyd, J., Schwarz, M., Patiño, S., Baker, T. R., Czimczik, C., Fyllas, N. M., Martinelli,
939 L., Nardoto, G. B., Schmerler, J., Santos, A. J. B., Hodnett, M. G., Herrera, R., Luizão, F. J., Arneth, A.,
940 Lloyd, G., Dezzeo, N., Hilke, I., Kuhlmann, I., Raessler, M., Brand, W. A., Geilmann, H., Moraes
941 Filho, J. O., Carvalho, F. P., Araujo Filho, R. N., Chaves, J. E., Cruz Junior, O. F., Pimentel, T. P. and
942 Paiva, R.: Variations in chemical and physical properties of Amazon forest soils in relation to their
943 genesis, Biogeosciences, 7(5), 1515–1541, 2010.

944 Quesada, C. A., Phillips, O. L., Schwarz, M., Czimczik, C. I., Baker, T. R., Patiño, S., Fyllas, N. M.,
945 Hodnett, M. G., Herrera, R., Almeida, S., Alvarez Dávila, E., Arneth, A., Arroyo, L., Chao, K. J.,
946 Dezzeo, N., Erwin, T., di Fiore, A., Higuchi, N., Honorio Coronado, E., Jimenez, E. M., Killeen, T.,
947 Lezama, A. T., Lloyd, G., López-González, G., Luizão, F. J., Malhi, Y., Monteagudo, A., Neill, D. A.,
948 Núñez Vargas, P., Paiva, R., Peacock, J., Peñuela, M. C., Peña Cruz, A., Pitman, N., Priante Filho, N.,
949 Prieto, A., Ramírez, H., Rudas, A., Salomão, R., Santos, A. J. B., Schmerler, J., Silva, N., Silveira, M.,
950 Vásquez, R., Vieira, I., Terborgh, J. and Lloyd, J.: Basin-wide variations in Amazon forest structure and
951 function are mediated by both soils and climate, Biogeosciences, 9(6), 2203–2246, 2012.

952 R Core Team (2014). R: A language and environment for statistical computing. R Foundation for
953 Statistical Computing, Vienna, Austria.

954 Raaimakers, D., Boot, R. G. A., Dijkstra, P. and Pot, S.: Photosynthetic rates in relation to leaf
955 phosphorus content in pioneer versus climax tropical rainforest trees, Oecologia, 102(1), 120–125,
956 1995.

957 Reich, P. B., Oleksyn, J. and Wright, I. J.: Leaf phosphorus influences the photosynthesis–nitrogen
958 relation: a cross-biome analysis of 314 species, Oecologia, 160(2), 207–212, 2009.

959 Reich, P. B., Tjoelker, M. G., Pregitzer, K. S., Wright, I. J., Oleksyn, J. and Machado, J.-L.: Scaling of
960 respiration to nitrogen in leaves, stems and roots of higher land plants, Ecology Letters, 11(8), 793–801,
961 2008.

962 Reich, P. B., Walters, M. B. and Ellsworth, D. S.: From tropics to tundra: global convergence in plant
963 functioning, Proceedings of the National Academy of Sciences, 94(25), 13730–13734, 1997.

964 Reich, P. B., Walters, M. B., Ellsworth, D. S. and Uhl, C.: Photosynthesis-nitrogen relations in
965 Amazonian tree species, Oecologia, 97(1), 62–72, 1994.

966 Ryan, M. G., Hubbard, R. M., Clark, D. A. and Sanford Jr, R. L.: Woody-tissue respiration for
967 Simarouba amara and Minquartia guianensis, two tropical wet forest trees with different growth habits,
968 Oecologia, 100(3), 213–220, 1994.

969 Scheiter, S. and Higgins, S. I.: Impacts of climate change on the vegetation of Africa: an adaptive
970 dynamic vegetation modelling approach, Global Change Biology, 15(9), 2224–2246, 2009.

971 Scheiter, S., Langan, L. and Higgins, S. I.: Next-generation dynamic global vegetation models: learning
972 from community ecology, New Phytol, 198(3), 957–969, 2013.

973 Sheffield, J., Goteti, G. and Wood, E. F.: Development of a 50-year high-resolution global dataset of
974 meteorological forcings for land surface modeling, Journal of Climate, 19(13), 3088–3111, 2006.

975 Shukla, J., Nobre, C. and Sellers, P.: Amazon deforestation and climate change, Science(Washington),
976 247(4948), 1322–1325, 1990.

977 Sitch, S., Smith, B., Prentice, I. C., Arneth, A., Bondeau, A., Cramer, W., Kaplan, J. O., Levis, S., Lucht,
978 W., Sykes, M. T., Thonicke, K. and Venevsky, S.: Evaluation of ecosystem dynamics, plant geography
979 and terrestrial carbon cycling in the LPJ dynamic global vegetation model, Global Change Biology, 9(2),
980 161–185, 2003.

981 Sombroek, W.: Amazon landforms and soils in relation to biological diversity, Acta Amazonica, 30(1),
982 81–100, 2000.

983 Sombroek, W.: Spatial and temporal patterns of Amazon rainfall: consequences for the planning of
984 agricultural occupation and the protection of primary forests, AMBIO: A Journal of the Human
985 Environment, 30(7), 388–396, 2001.

986 Spitters, C. J. T.: Separating the diffuse and direct component of global radiation and its implications
987 for modeling canopy photosynthesis Part II. Calculation of canopy photosynthesis, Agricultural and
988 Forest meteorology, 38(1), 231–242, 1986.

989 Spracklen, D. V., Arnold, S. R. and Taylor, C. M.: Observations of increased tropical rainfall preceded
990 by air passage over forests, Nature, 489(7415), 282–285, 2012.

991 Sultan, S. E.: Phenotypic plasticity for plant development, function and life history, Trends in plant
992 science, 5(12), 537–542, 2000.

993 Taylor, M. S. and Thompson, J. R.: A data based algorithm for the generation of random vectors,
994 Computational Statistics & Data Analysis, 4(2), 93–101, 1986.

995 Ter Steege, H., Pitman, N. C. A., Phillips, O. L., Chave, J., Sabatier, D., Duque, A., Molino, J.-F.,
996 Prévost, M.-F., Spichiger, R., Castellanos, H., von Hildebrand, P. and Vásquez, R.: Continental-scale
997 patterns of canopy tree composition and function across Amazonia, Nature, 443(7110), 444–447, 2006.

998 Ter Steege, H. ter, Pitman, N. C. A., Sabatier, D., Baraloto, C., Salomão, R. P., Guevara, J. E., Phillips,
999 O. L., Castilho, C. V., Magnusson, W. E., Molino, J.-F., Monteagudo, A., Vargas, P. N., Montero, J. C.,
1000 Feldpausch, T. R., Coronado, E. N. H., Killeen, T. J., Mostacedo, B., Vasquez, R., Assis, R. L.,
1001 Terborgh, J., Wittmann, F., Andrade, A., Laurance, W. F., Laurance, S. G. W., Marimon, B. S.,
1002 Marimon, B.-H., Vieira, I. C. G., Amaral, I. L., Brienen, R., Castellanos, H., López, D. C.,
1003 Duivenvoorden, J. F., Mogollón, H. F., Matos, F. D. de A., Dávila, N., García-Villacorta, R., Diaz, P. R.
1004 S., Costa, F., Emilio, T., Levis, C., Schietti, J., Souza, P., Alonso, A., Dallmeier, F., Montoya, A. J. D.,
1005 Piedade, M. T. F., Araujo-Murakami, A., Arroyo, L., Gribel, R., Fine, P. V. A., Peres, C. A., Toledo, M.,
1006 C, G. A. A., Baker, T. R., Cerón, C., Engel, J., Henkel, T. W., Maas, P., Petronelli, P., Stropp, J.,
1007 Zartman, C. E., Daly, D., Neill, D., Silveira, M., Paredes, M. R., Chave, J., Filho, D. de A. L., Jørgensen,
1008 P. M., Fuentes, A., Schöngart, J., Valverde, F. C., Fiore, A. D., Jimenez, E. M., Mora, M. C. P., Phillips,
1009 J. F., Rivas, G., Andel, T. R. van, Hildebrand, P. von, Hoffman, B., Zent, E. L., Malhi, Y., Prieto, A.,
1010 Rudas, A., Ruschell, A. R., Silva, N., Vos, V., Zent, S., Oliveira, A. A., Schutz, A. C., Gonzales, T.,
1011 Nascimento, M. T., Ramirez-Angulo, H., Sierra, R., Tirado, M., Medina, M. N. U., Heijden, G. van der,
1012 Vela, C. I. A., Torre, E. V., Vriesendorp, C., et al.: Hyperdominance in the Amazonian Tree Flora,
1013 Science, 342(6156), 2013.

1014 Thompson, J. R.: Empirical Model Building, John Wiley & Sons., 1989.

1015 Tjoelker, M. G., Oleksyn, J. and Reich, P. B.: Modelling respiration of vegetation: evidence for a general
1016 temperature-dependent Q10, Global Change Biology, 7(2), 223–230, 2001.

1017 Townsend, A. R., Asner, G. P. and Cleveland, C. C.: The biogeochemical heterogeneity of tropical
1018 forests, Trends in Ecology & Evolution, 23(8), 424–431, 2008.

1019 Valentini, R., Matteucci, G., Dolman, A. J., Schulze, E.-D., Rebmann, C., Moors, E. J., Granier, A.,
1020 Gross, P., Jensen, N. O., Pilegaard, K., Lindroth, A., Grelle, A., Bernhofer, C., Grünwald, T., Aubinet,
1021 M., Ceulemans, R., Kowalski, A. S., Vesala, T., Rannik, Ü., Berbigier, P., Loustau, D., Guðmundsson,
1022 J., Thorgeirsson, H., Ibrom, A., Morgenstern, K., Clement, R., Moncrieff, J., Montagnani, L., Minerbi,
1023 S. and Jarvis, P. G.: Respiration as the main determinant of carbon balance in European forests,
1024 Nature, 404(6780), 861–865, 2000.

1025 Verheijen, L. M., Brovkin, V., Aerts, R., Bönisch, G., Cornelissen, J. H. C., Kattge, J., Reich, P. B.,
1026 Wright, I. J. and van Bodegom, P. M.: Impacts of trait variation through observed trait–climate
1027 relationships on performance of an Earth system model: a conceptual analysis, Biogeosciences, 10(8),
1028 5497–5515, 2013.

1029 Visual Numerics Fortran Numerical Stat Library, 2014 (available at
1030 http://www.roguewave.com/portals/0/products/imsl-numerical-libraries/fortran-
1031 library/docs/7.0/stat/stat.htm)

1032 Vitousek, P. M. and Farrington, H.: Nutrient limitation and soil development: experimental test of a
1033 biogeochemical theory, Biogeochemistry, 37(1), 63–75, 1997.

1034 Walker, T. W. and Syers, J. K.: The fate of phosphorus during pedogenesis, Geoderma, 15(1), 1–19,
1035 1976.

1036 Wang, Y. P., Lu, X. J., Wright, I. J., Dai, Y. J., Rayner, P. J. and Reich, P. B.: Correlations among leaf
1037 traits provide a significant constraint on the estimate of global gross primary production, Geophysical
1038 Research Letters, 2012.

1039 White, A., Cannell, M. G. and Friend, A. D.: Climate change impacts on ecosystems and the terrestrial
1040 carbon sink: a new assessment, Global Environmental Change, 9, S21–S30, 1999.

1041 Wright, I. J., Reich, P. B., Westoby, M., Ackerly, D. D., Baruch, Z., Bongers, F., Cavender-Bares, J.,
1042 Chapin, T., Cornelissen, J. H. C., Diemer, M., Flexas, J., Garnier, E., Groom, P. K., Gulias, J.,
1043 Hikosaka, K., Lamont, B. B., Lee, T., Lee, W., Lusk, C., Midgley, J. J., Navas, M.-L., Niinemets, Ü.,
1044 Oleksyn, J., Osada, N., Poorter, H., Poot, P., Prior, L., Pyankov, V. I., Roumet, C., Thomas, S. C.,
1045 Tjoelker, M. G., Veneklaas, E. J. and Villar, R.: The worldwide leaf economics spectrum, Nature,
1046 428(6985), 821–827, 2004.

1047 York, D., Evensen, N. M., Martínez, M. L. and Delgado, J. D. B.: Unified equations for the slope,
1048 intercept, and standard errors of the best straight line, American Journal of Physics, 72, 367, 2004.

1049 Zhang, Y., Xu, M., Chen, H. and Adams, J.: Global pattern of NPP to GPP ratio derived from MODIS
1050 data: effects of ecosystem type, geographical location and climate, Global Ecology and Biogeography,
1051 18(3), 280–290, 2009.
1052

Tables & Figures

Table 1. Kendall correlation coefficients (τ) and associated significance levels (p) between simulated gross primary productivity (Π_G), net primary productivity (Π_N), carbon use efficiency (C_U) and key environmental factors.

	Π_G(kgC m^{-2} y^{-1})	Π_N(kgC m^{-2} y^{-1})	C_U (-)
Mean Annual Temperature - T_A (°C)	τ = -0.17 p = 0.131	τ = -0.21 p = 0.065	τ = -0.11 p = 0.33
Annual Precipitation P_A(mm)	**τ = 0.54** p < 0.001	**τ = 0.60** p < 0.001	**τ = 0.36** p = 0.002
Soil nutrient availability Φ_1 (PCA Axis 1)	**τ = 0.48** p < 0.001	**τ = 0.50** p < 0.001	**τ = 0.39** p < 0.001

Figure Captions

Figure 1: The five basic components of the model and information flow among them. Tree by tree traits and size initialisation takes place at the beginning of each simulation. Carbon and water fluxes, as well as gross and net primary productivity are estimated daily.

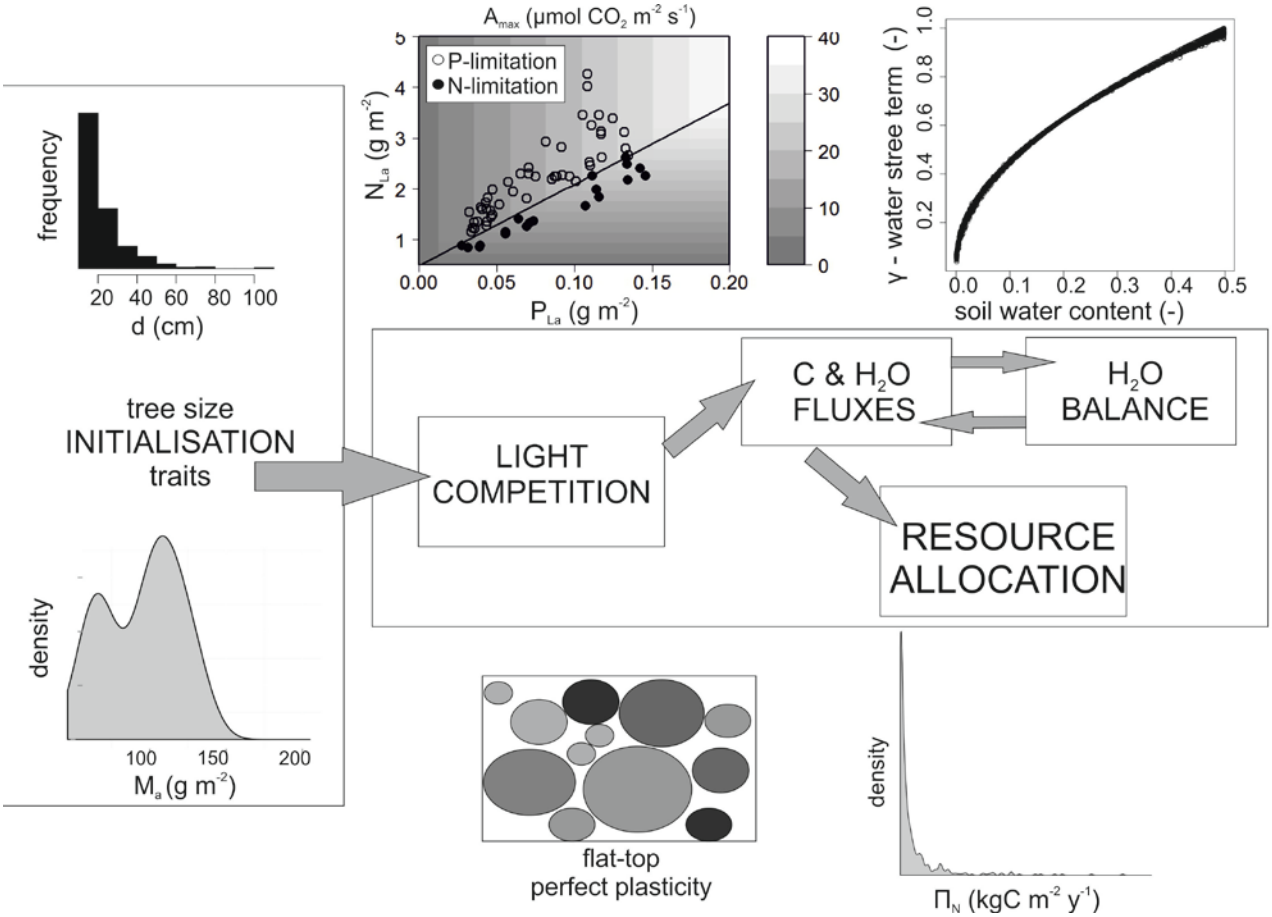

Figure 2. Geographic distribution of study sites. Dark grey triangles indicate the three eddy flux tower sites (with local names), light gray circles indicate the seven intensive measurement plots (with plot codes), and crosses indicate the coordinates of the 40 RAINFOR permanent measurement plots.

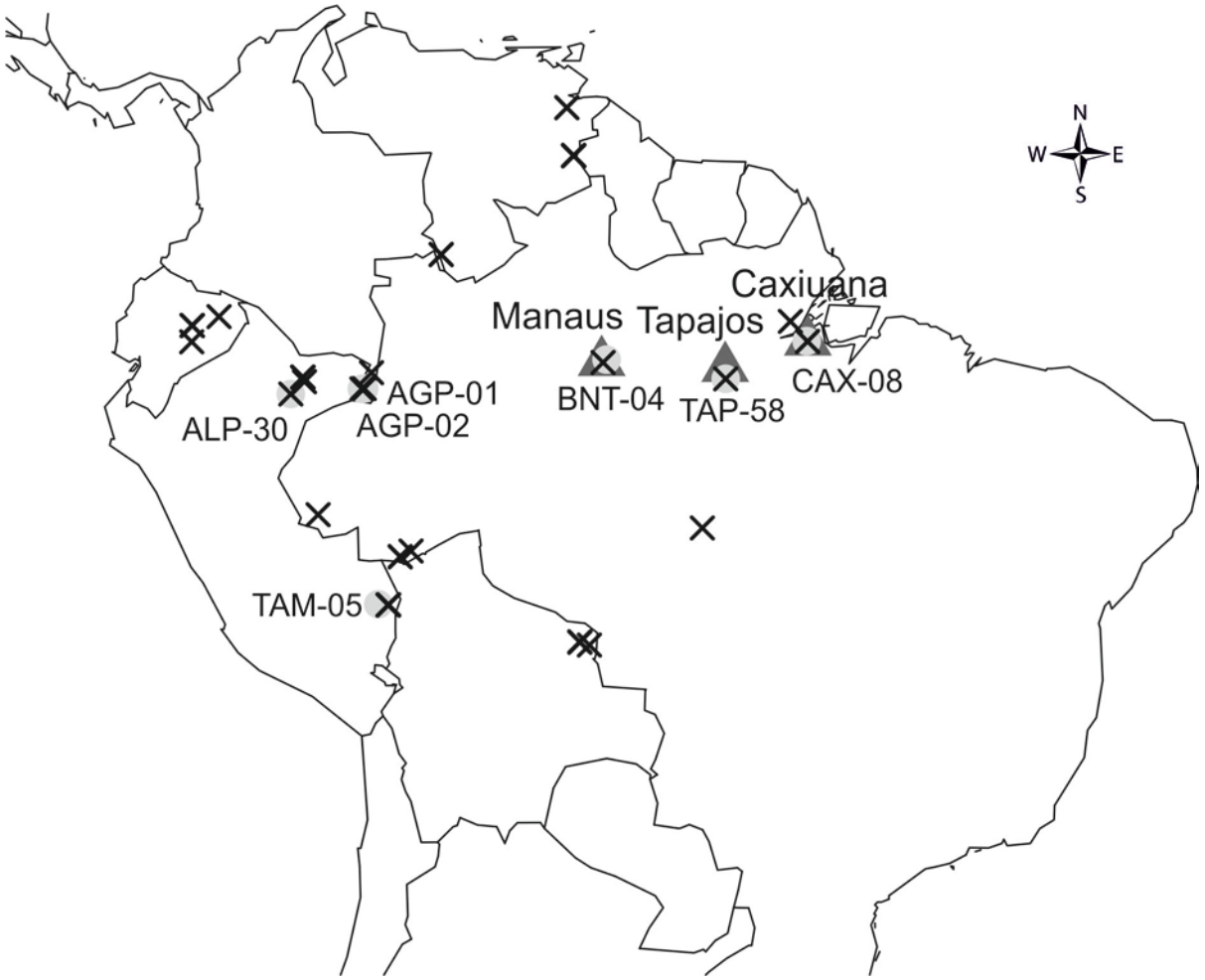

Figure 3: Simulated against observed mean daily canopy conductance G_C for the three sites with eddy flux data. The broken line represents an 1:1 relationship and the continuous line illustrates a standardised major axis (SMA) regression.

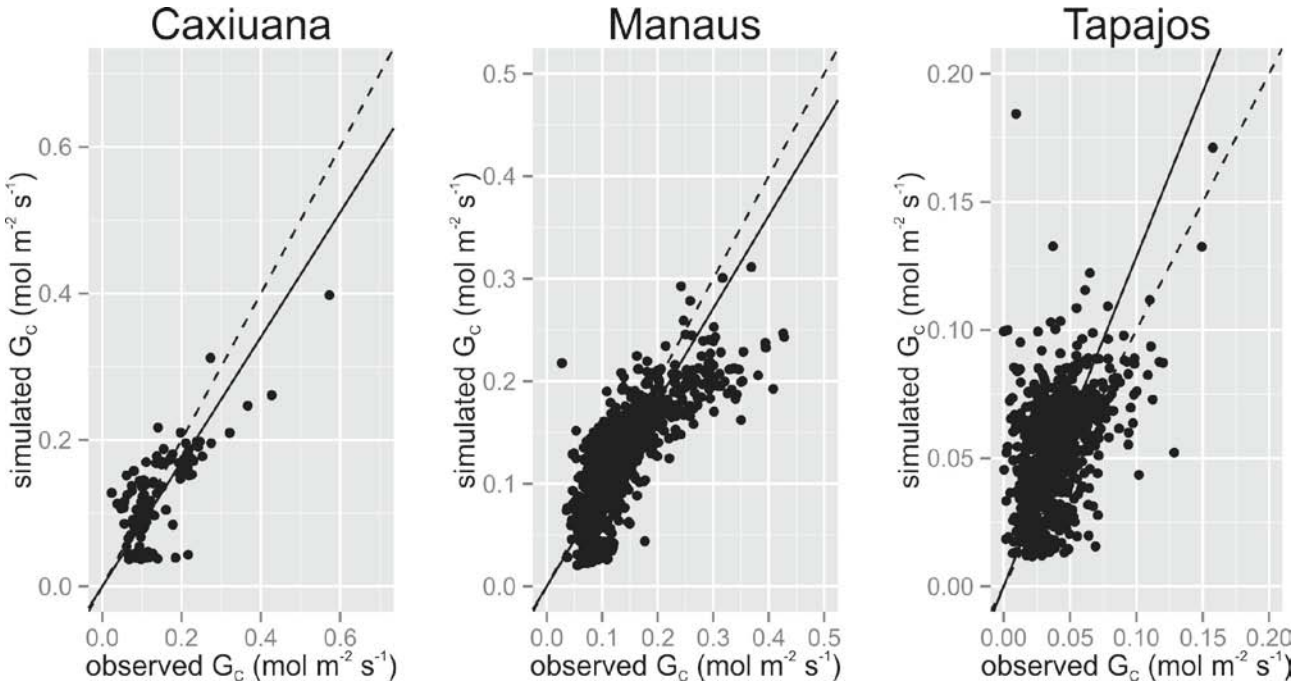

Figure 4: Simulated stem growth rate $\Pi_{N,s}$ against observed aboveground biomass change ΔB_{ABG} for different size classes for the 2000-2006 period. Upper panel: infertile plots. Lower panel: fertile plots. The broken line represents an 1:1 relationship continuous. The continuous line illustrates the straight line fit using the York method (see text for details).

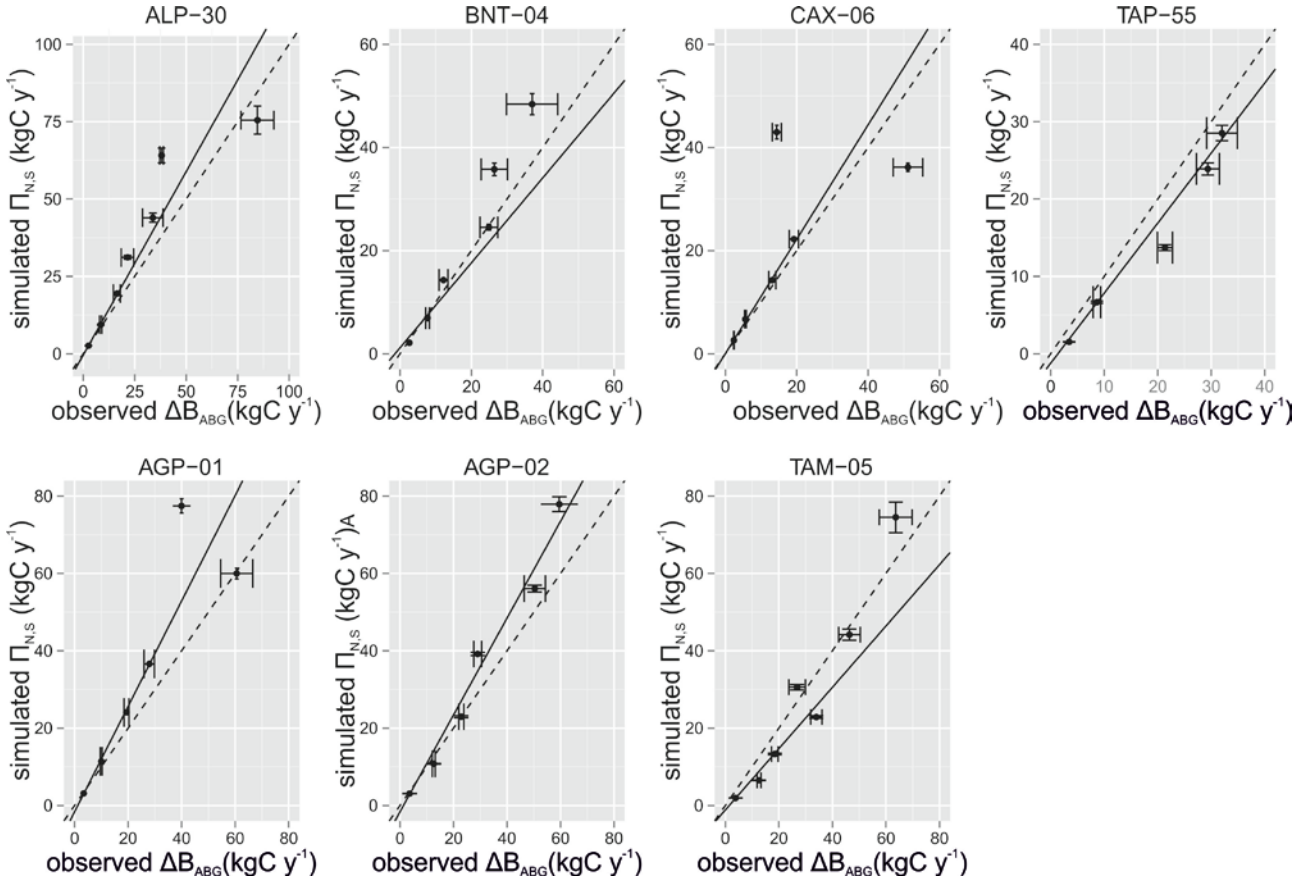

1081 Figure 5: Simulated stand-level aboveground net primary productivity (Π_{AN}) against observed stand-
1082 level aboveground biomass growth (ΔB_{ABG}) of surviving trees, at the 40 PM plots. The line illustrates a
1083 SMA regression of α=0.92 (0.72...1.18) and R^2=0.42. Red dots indicate high nutrient availability and
1084 blue dots indicate low nutrient availability plots.

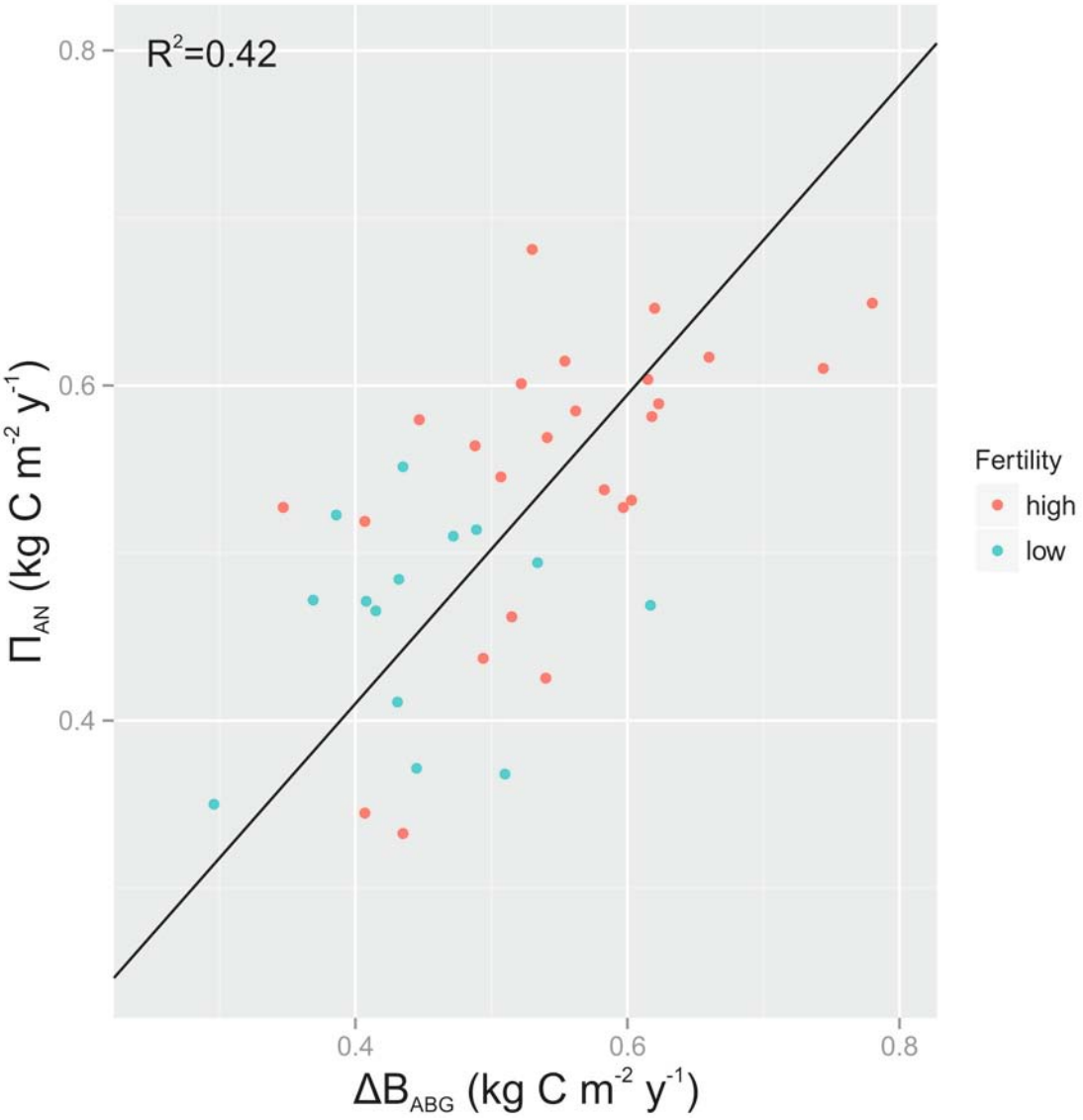

1085

Figure 6: Summary of the randomisation exercise simulations. a) Simulated stand-level aboveground net primary productivity (Π_{AN}) against observed stand-level aboveground biomass growth (ΔB_{ABG}) for the four different set-ups. The slope of the SMA (a) and the adjusted R^2 are given in the parentheses for each set-up. Different colours indicate different setups b) Simulated Amazon-wide aboveground net primary productivity (Π_{AN}) for the four different set-ups.